Bulletin of the Institute of Mathematics
Academia Sinica (New Series)
Vol. **2** (2007), No. 2, pp. 495-532

ENERGY AND CHEMICAL POTENTIAL ASYMPTOTICS FOR THE GROUND STATE OF BOSE-EINSTEIN CONDENSATES IN THE SEMICLASSICAL REGIME

BY

WEIZHU BAO, FONG YIN LIM AND YANZHI ZHANG

Abstract

Asymptotic approximations for the energy and chemical potential of the ground state in Bose-Einstein condensates are presented in the semiclassical regime with several typical trapping potentials. As preparatory steps, we begin with the three-dimensional (3D) Gross-Pitaevskii equation (GPE), review several typical external trapping potentials, scale the 3D GPE and show how to reduce it to 1D and 2D GPEs in certain limiting trapping frequency regime. For the 1D box potential, we derive asymptotic approximations up to $o(1)$ in term of the scaled interacting parameter β_d for energy and chemical potential of the ground and all excited states in both weakly interacting regime, i.e. $\beta_d \to 0$ and strongly repulsive interacting regime, i.e. $\beta_d \to \infty$, respectively. For the 1D harmonic oscillator, double well and optical lattice potentials, as well as a more general external potential in high dimensions, we get asymptotic approximations up to $o(1)$ in term of the scaled interacting parameter β_d for the energy and chemical potential of the ground state in semiclassical regime, i.e. $\beta_d \to \infty$. Our extensive numerical results confirm all our asymptotic approximations, provide convergence rate and suggest several very interesting conclusions.

Received December 9, 2004 and in revised form March 29, 2005.

AMS Subject Classification: 35B40, 35P30, 65N06, 65N25, 81V45.

Key words and phrases: Bose-Einstein condensation, Gross-Pitaevskii equation, box potential, energy, chemical potential, harmonic oscillator potential, double well potential, optical lattice potential, ground state, excited state, semiclassical regime.

1. Introduction

Recent experimental advances in achieving and observing Bose-Einstein condensation (BEC) in trapped neutral atomic vapors [3, 25] have spurred great excitement in the atomic physics community and renewed the interest in studying the collective dynamics of macroscopic ensembles of atoms occupying the same one-particle quantum state [24, 39, 41]. Theoretical predictions of the properties of a BEC like the density profile [13], collective excitations [27, 31] and the formation of vortices [26, 42] can now be compared with experimental data [1, 3, 32]. Needless to say that this dramatic progress on the experimental front has stimulated a wave of activity on both the theoretical and the numerical front.

The properties of a BEC at temperatures T much smaller than the critical condensation temperature T_c [33] are usually well modeled by a nonlinear Schrödinger equation (NLSE) for the macroscopic wave function [29, 33, 40] known as the Gross-Pitaevskii equation (GPE) [29, 40], which incorporates the trap potential as well as the interactions among the atoms. The effect of the interactions is described by a mean field which leads to a nonlinear term in the GPE. The cases of repulsive and attractive interactions - which can both be realized in the experiment - correspond to defocusing and focusing nonlinearities in the GPE, respectively. The results obtained by solving the GPE showed excellent agreement with most of the experiments (for a review see [4, 23]). Thus theoretical and numerical study of GPE is very important in understanding BEC.

There has been a series of recent theoretical and numerical studies for understanding BEC. From theoretical point of view, we refer to the study for properties of the energy functional [24, 35, 36, 41], Thomas-Fermi (TF) approximation [8, 11], vortex formation [12, 39, 41], solutions of time-independent and time-dependent GPE [36, 41], etc. From numerical point of view, we refer to the study for developing efficient and stable numerical methods to compute ground state [6, 11, 18, 20, 21] and dynamics of BEC [7, 8, 10, 19], simulating BEC in 3D [9] and multi-component [5, 20], comparing with experimental data [3, 28], etc. Currently, several important problems are still open in this field, especially in the semicalssical regime. For example, (i) Does the minimizer of the energy functional for GPE correspond to the minimum chemical potential? (ii) What is the convergence rate of the TF approximation? (iii) What is the ratio between the energy and chemical potential when the scaled interacting parameter $\beta_d \to \infty$? (iv) What is the

width of the boundary or interior layers in ground or excited states? (v) Is there an asymptotic formula for the energy and chemical potential when the number of atoms in the condensate is very large? In this paper, we will study these questions by using asymptotic and numerical methods. Since the experiments are usually done with thousands to millions atoms, i.e. in the semiclassical regime, we will mainly focus ourselves in this regime. For box potential, we obtain asymptotic approximations up to $o(1)$ in term of the scaled interacting parameter β_d for energy and chemical potential of the ground and all excited states by applying a matched asymptotic method. For the 1D harmonic oscillator, double well and optical lattice potentials, as well as a more general external potential in high dimensions, we derive asymptotic approximations up to $o(1)$ in term of β_d for the energy and chemical potential of the ground state by carefully studying the TF approximation. These asymptotic approximations are confirmed by our extensive numerical results and convergence rates are also reported.

The paper is organized as follows. In Section 2 we start out with the 3D GPE, review several typical external trapping potentials, scale the 3D GPE and show how to reduce it to lower dimensions. In Section 3 we present TF and matched asymptotic approximations for the ground state and all excited states, as well as their energy and chemical potential with a 1D box potential. In Section 4 we get asymptotic approximations for the energy and chemical potential of the ground state with nonuniform potentials. Finally, some conclusions are drawn in Section 5.

2. The Gross-Pitaevskii Equation

At temperature T much smaller than the critical temperature T_c [33], a BEC is well described by the macroscopic wave function $\psi(\mathbf{x}, t)$ whose evolution is governed by a self-consistent, mean field nonlinear Schrödinger equation (NLSE) known as the Gross- Pitaevskii equation (GPE) [29, 40]

$$\begin{aligned} i\hbar\frac{\partial\psi(\mathbf{x},t)}{\partial t} &= \frac{\delta E(\psi)}{\delta\psi^*} := H\ \psi \\ &= -\frac{\hbar^2}{2m}\nabla^2\psi(\mathbf{x},t) + V(\mathbf{x})\psi(\mathbf{x},t) + NU_0|\psi(\mathbf{x},t)|^2\psi(\mathbf{x},t), \quad (2.1) \end{aligned}$$

where $\mathbf{x} = (x, y, z)^T$ is the spatial coordinate vector, m is the atomic mass, $\hbar$ is the Planck constant, N is the number of atoms in the condensate, $U_0 = 4\pi\hbar^2 a_s/m$ describes the interactions between atoms in the condensate

with a_s the atomic scattering length (positive for repulsive interaction and negative for attractive interaction), $V(\mathbf{x})$ is an external trapping potential, and the energy functional $E(\psi)$ is defined as

$$E(\psi) = \int_{\mathbb{R}^3} \left[\frac{\hbar^2}{2m} |\nabla \psi|^2 + V(\mathbf{x}) |\psi|^2 + \frac{NU_0}{2} |\psi|^4 \right] d\mathbf{x}. \tag{2.2}$$

Here we use f^* denotes the conjugate of a function f. It is convenient to normalize the wave function by requiring

$$\|\psi(\cdot, t)\|^2 := \int_{\mathbb{R}^3} |\psi(\mathbf{x}, t)|^2 d\mathbf{x} = 1. \tag{2.3}$$

2.1. Different external trapping potentials

In the early BEC experiments, a single harmonic oscillator well was used to trap the atoms in the condensate [14, 24]. Recently more advanced and complicated traps are applied in studying BEC in laboratory [15, 18, 38, 41]. In this subsection, we review several typical trapping potentials which are widely used in current experiments.

I. Three-dimensional (3D) harmonic oscillator potential [41]:

$$V_{\rm ho}(\mathbf{x}) = V_{\rm ho}(x) + V_{\rm ho}(y) + V_{\rm ho}(z), \ \mathbf{x} \in \mathbb{R}^3, \ V_{\rm ho}(\tau) = \frac{m}{2} \omega_\tau^2 \tau^2, \ \tau = x, y, z, \tag{2.4}$$

where ω_x, ω_y and ω_z are the trap frequencies in x-, y- and z-direction respectively.

II. 2D harmonic oscillator + 1D double-well potential (Type I) [38]:

$$V_{\rm dw}^{(1)}(\mathbf{x}) = V_{\rm dw}^{(1)}(x) + V_{\rm ho}(y) + V_{\rm ho}(z), \ \mathbf{x} \in \mathbb{R}^3, \ V_{\rm dw}^{(1)}(x) = \frac{m}{2} \nu_x^4 \left(x^2 - \hat{a}^2 \right)^2, \tag{2.5}$$

where $\pm\hat{a}$ are the double-well centers in x-axis, ν_x is a given constant with physical dimension $1/[\text{s m}]^{1/2}$.

III. 2D harmonic oscillator + 1D double-well potential (Type II) [16, 30]:

$$V_{\rm dw}^{(2)}(\mathbf{x}) = V_{\rm dw}^{(2)}(x) + V_{\rm ho}(y) + V_{\rm ho}(z), \ \mathbf{x} \in \mathbb{R}^3, \ V_{\rm dw}^{(2)}(x) = \frac{m}{2} \omega_x^2 \left(|x| - \hat{a} \right)^2. \tag{2.6}$$

IV. 3D harmonic oscillator + optical lattice potential [2, 22, 41]:

$$V_{\rm hop}(\mathbf{x}) = V_{\rm ho}(\mathbf{x}) + V_{\rm opt}(x) + V_{\rm opt}(y) + V_{\rm opt}(z),\ \mathbf{x} \in \mathbb{R}^3,\ V_{\rm opt}(\tau) = S_\tau\ E_\tau \sin^2(\hat{q}_\tau \tau), \tag{2.7}$$

where $\hat{q}_\tau = 2\pi/\lambda_\tau$ is fixed by the wavelength λ_τ of the laser light creating the stationary 1D lattice wave, $E_\tau = \hbar^2 \hat{q}_\tau^2/2m$ is the so-called recoil energy, and S_τ is a dimensionless parameter providing the intensity of the laser beam. The optical lattice potential has periodicity $T_\tau = \pi/\hat{q}_\tau = \lambda_\tau/2$ along τ-axis $(\tau = x, y, z)$.

V. 3D box potential [41]:

$$V_{\rm box}(\mathbf{x}) = \begin{cases} 0, & 0 < x, y, z < L, \\ \infty, & \text{otherwise.} \end{cases} \tag{2.8}$$

where L is the length of the box in the x-, y-, z-direction.

For more types of external trapping potential, we refer to [39, 41].

2.2. Dimensionless GPE

In order to scale Eq. (2.1) under the normalization (2.3), we introduce

$$\tilde{t} = \frac{t}{t_0}, \quad \tilde{\mathbf{x}} = \frac{\mathbf{x}}{x_0}, \quad \tilde{\psi}\left(\tilde{\mathbf{x}}, \tilde{t}\right) = x_0^{3/2} \psi\left(\mathbf{x}, t\right), \quad \tilde{E}(\tilde{\psi}) = \frac{E(\psi)}{E_0}, \tag{2.9}$$

where t_0, x_0 and E_0 are the scaling parameters of dimensionless time, length and energy units, respectively. Plugging (2.9) into (2.1), multiplying by $t_0^2/m x_0^{1/2}$, and then removing all $\tilde{}$, we obtain the following dimensionless GPE under the normalization (2.3) in 3D:

$$\begin{aligned} i\frac{\partial \psi(\mathbf{x}, t)}{\partial t} &= \frac{\delta E(\psi)}{\delta \psi^*} := H\ \psi \\ &= -\frac{1}{2}\nabla^2 \psi(\mathbf{x}, t) + V(\mathbf{x})\psi(\mathbf{x}, t) + \beta |\psi(\mathbf{x}, t)|^2 \psi(\mathbf{x}, t), \end{aligned} \tag{2.10}$$

where the dimensionless energy functional $E(\psi)$ is defined as

$$E(\psi) = \int_{\mathbb{R}^3} \left[\frac{1}{2}|\nabla \psi|^2 + V(\mathbf{x})|\psi|^2 + \frac{\beta}{2}|\psi|^4 \right] d\mathbf{x}, \tag{2.11}$$

and the choices for the scaling parameters t_0 and x_0, the dimensionless potential $V(\mathbf{x})$ with $\gamma_y = t_0 \omega_y$ and $\gamma_z = t_0 \omega_z$, the energy unit $E_0 = \hbar/t_0 =$

$\hbar^2/mx_0^2$, and the interaction parameter $\beta = 4\pi a_s N/x_0$ for different external trapping potentials are given below [37]:

I. 3D harmonic oscillator potential:

$$t_0 = \frac{1}{\omega_x}, \quad x_0 = \sqrt{\frac{\hbar}{m\omega_x}}, \quad V(\mathbf{x}) = \frac{1}{2}\left(x^2 + \gamma_y^2 y^2 + \gamma_z^2 z^2\right).$$

II. 2D harmonic oscillator + 1D double-well potential (type I):

$$t_0 = \left(\frac{m}{\hbar\nu_x^4}\right)^{1/3}, \ x_0 = \left(\frac{\hbar}{m\nu_x^2}\right)^{1/3}, \ a = \frac{\hat{a}}{x_0}, \ V(\mathbf{x}) = \frac{1}{2}\left[\left(x^2 - a^2\right)^2 + \gamma_y^2 y^2 + \gamma_z^2 z^2\right].$$

III. 2D harmonic oscillator + 1D double-well potential (type II):

$$t_0 = \frac{1}{\omega_x}, \quad x_0 = \sqrt{\frac{\hbar}{m\omega_x}}, \quad a = \frac{\hat{a}}{x_0}, \quad V(\mathbf{x}) = \frac{1}{2}\left[(|x| - a)^2 + \gamma_y^2 y^2 + \gamma_z^2 z^2\right].$$

IV. 3D harmonic oscillator + optical lattice potentials:

$$t_0 = \frac{1}{\omega_x}, \quad x_0 = \sqrt{\frac{\hbar}{m\omega_x}}, \quad k_\tau = \frac{2\pi^2 x_0^2 S_\tau}{\lambda_\tau^2}, \quad q_\tau = \frac{2\pi x_0}{\lambda_\tau}, \quad \tau = x, y, z,$$
$$V(\mathbf{x}) = \frac{1}{2}(x^2 + \gamma_y^2 y^2 + \gamma_z^2 z^2) + k_x \sin^2(q_x x) + k_y \sin^2(q_y y) + k_z \sin^2(q_z z).$$

V. 3D Box potential:

$$t_0 = \frac{mL^2}{\hbar}, \quad x_0 = L, \quad V(\mathbf{x}) = \begin{cases} 0, & 0 < x, y, z < 1, \\ \infty, & \text{otherwise.} \end{cases}$$

Under the external potentials I–IV, when $\omega_y \approx 1/t_0$ and $\omega_z \gg 1/t_0$ ($\Leftrightarrow$ $\gamma_y \approx 1$ and $\gamma_z \gg 1$), i.e. a disk-shape condensation, following the procedure used in [8, 11, 34], the 3D GPE can be reduced to a 2D GPE. Similarly, when $\omega_y \gg 1/t_0$ and $\omega_z \gg 1/t_0$ ($\Leftrightarrow$ $\gamma_y \gg 1$ and $\gamma_z \gg 1$), i.e. a cigar-shaped condensation, the 3D GPE can be reduced to a 1D GPE [8, 11, 34]. These suggest us to consider a GPE in d-dimension ($d = 1, 2, 3$):

$$i\,\partial_t \psi(\mathbf{x}, t) = -\frac{1}{2}\Delta\psi + V_d(\mathbf{x})\psi + \beta_d|\psi|^2\psi, \qquad \mathbf{x} \in \Omega \subseteq \mathbb{R}^d, \tag{2.12}$$
$$\psi(\mathbf{x}, t) = 0, \qquad \mathbf{x} \in \Gamma = \partial\Omega, \tag{2.13}$$

$$\psi(\mathbf{x},0)=\psi_0(\mathbf{x}),\qquad \mathbf{x}\in\Omega; \tag{2.14}$$

where β_d is the scaled interacting parameter and $V_d(\mathbf{x})$ is the scaled external potential.

There are two important invariants of (2.12): the normalization of the wave function

$$N(\psi)=\int_\Omega |\psi(\mathbf{x},t)|^2\,d\mathbf{x}\equiv N(\psi_0)=\int_\Omega |\psi_0(\mathbf{x})|^2\,d\mathbf{x}=1,\quad t\geq 0 \tag{2.15}$$

and the energy functional

$$E(\psi)=\int_\Omega\left[\frac{1}{2}|\nabla\psi|^2+V_d(\mathbf{x})|\psi|^2+\frac{\beta_d}{2}|\psi|^4\right]d\mathbf{x}\equiv E(\psi_0),\quad t\geq 0. \tag{2.16}$$

In fact, the energy functional $E(\psi)$ can be split into three parts, i.e. kinetic energy $E_{\rm kin}(\psi)$, potential energy $E_{\rm pot}(\psi)$ and interaction energy $E_{\rm int}(\psi)$, which are defined as

$$E_{\rm int}(\psi) = \int_\Omega \frac{\beta_d}{2}|\psi(\mathbf{x},t)|^4 d\mathbf{x},\quad E_{\rm pot}(\psi)=\int_\Omega V_d(\mathbf{x})|\psi(\mathbf{x},t)|^2 d\mathbf{x}, \tag{2.17}$$

$$E_{\rm kin}(\psi) = \int_\Omega \frac{1}{2}|\nabla\psi(\mathbf{x},t)|^2\,d\mathbf{x},\ E(\psi)=E_{\rm kin}(\psi)+E_{\rm pot}(\psi)+E_{\rm int}(\psi). \tag{2.18}$$

2.3. Stationary states

To find the stationary solution of (2.12), we write

$$\psi(\mathbf{x},t)=\phi(\mathbf{x})\,e^{-i\mu t}, \tag{2.19}$$

where μ is the chemical potential of the condensate and $\phi(\mathbf{x})$ is a function independent of time. Substituting (2.19) into (2.12) gives the following equation for $(\mu,\phi(\mathbf{x}))$:

$$\mu\,\phi(\mathbf{x})=-\frac{1}{2}\Delta\phi(\mathbf{x})+V_d(\mathbf{x})\phi(\mathbf{x})+\beta_d|\phi(\mathbf{x})|^2\phi(\mathbf{x}),\quad \mathbf{x}\in\Omega, \tag{2.20}$$

$$\phi(\mathbf{x})|_{\Gamma=\partial\Omega}=0, \tag{2.21}$$

under the normalization condition

$$\|\phi\|^2:=\int_\Omega |\phi(\mathbf{x})|^2 d\mathbf{x}=1. \tag{2.22}$$

This is a nonlinear eigenvalue problem with a constraint and any eigenvalue μ can be computed from its corresponding eigenfunction $\phi(\mathbf{x})$ by

$$\begin{aligned}\mu &= \mu(\phi) = \int_\Omega \left[\frac{1}{2}|\nabla\phi(\mathbf{x})|^2 + V_d(\mathbf{x})|\phi(\mathbf{x})|^2 + \beta_d|\phi(\mathbf{x})|^4\right] d\mathbf{x} \\ &= E(\phi) + \int_\Omega \frac{\beta_d}{2}|\phi(\mathbf{x})|^4 d\mathbf{x} = E(\phi) + E_{\rm int}(\phi). \end{aligned} \tag{2.23}$$

The ground state of a BEC is usually defined as the minimizer of the following minimization problem:

Find $(\mu_g, \phi_g \in S)$ such that

$$E_g := E(\phi_g) = \min_{\phi\in S} E(\phi), \qquad \mu_g := \mu(\phi_g) = E(\phi_g) + E_{\rm int}(\phi_g), \tag{2.24}$$

where $S = \{\phi \mid \|\phi\| = 1,\ E(\phi) < \infty\}$ is the unit sphere. When $\beta_d \geq 0$ and Ω is bounded or $\lim_{|\mathbf{x}|\to\infty} V(\mathbf{x}) = \infty$, there exists a unique positive minimizer of the minimization problem (2.24) [36].

It is easy to show that the ground state ϕ_g is an eigenfunction of the nonlinear eigenvalue problem. Any eigenfunction of (2.20) whose energy is larger than that of the ground state is usually called as excited states in the physics literatures. In the following, we always use $E_g = E(\phi_g)$, $E_{{\rm int},g} = E_{\rm int}(\phi_g)$, $E_{{\rm pot},g} = E_{\rm pot}(\phi_g)$, $E_{{\rm kin},g} = E_{\rm kin}(\phi_g)$ and $\mu_g = \mu(\phi_g)$ to denote the energy, interaction energy, potential energy, kinetic energy and chemical potential of the ground state ϕ_g respectively. Similarly, we use $E_k = E(\phi_k)$, $E_{{\rm int},k} = E_{\rm int}(\phi_k)$, $E_{{\rm pot},k} = E_{\rm pot}(\phi_k)$, $E_{{\rm kin},k} = E_{\rm kin}(\phi_k)$ and $\mu_k = \mu(\phi_k)$ to denote the corresponding quantities for the kth excited state ϕ_k.

In order to verify our asymptotic approximations provided in the next two sections numerically, we always solve the minimization problem (2.24) by a continuous normalized gradient flow (CNGF) with a backward Euler finite difference (BEFD) discretization proposed in [6] to compute the ground and excited states.

2.4. Semiclassical scaling and leading asymptotics

When $\Omega = \mathbb{R}^d$, $\beta_d \gg 1$ and $V_d(\mathbf{x}) = V_0(\mathbf{x}) + W(\mathbf{x})$ satisfying

$$V_0(\mathbf{x}) = \frac{1}{2}(\gamma_1^\alpha|x_1|^\alpha + \cdots + \gamma_d^\alpha|x_d|^\alpha), \qquad \lim_{|\mathbf{x}|\to\infty} \frac{W(\mathbf{x})}{V_0(\mathbf{x})} = 0, \tag{2.25}$$

with $\mathbf{x} = (x_1, \ldots, x_d)^T$, $\alpha > 0$, $0 < \gamma_j$, $1 \le j \le d$, another scaling (under the normalization (2.15) with ψ replacing by ψ^ε) for (2.12) is also very useful in practice by choosing $t \to t\varepsilon^{(\alpha-2)/(\alpha+2)}$, $\mathbf{x} \to \mathbf{x}\varepsilon^{-2/(2+\alpha)}$ and $\psi = \psi^\varepsilon\ \varepsilon^{d/(2+\alpha)}$ with $\varepsilon = 1/\beta_d^{(\alpha+2)/2(d+\alpha)}$:

$$\begin{aligned} i\varepsilon\frac{\partial\psi^\varepsilon(\mathbf{x},t)}{\partial t} &= \frac{\delta E^\varepsilon(\psi^\varepsilon)}{\delta(\psi^\varepsilon)^*} := H^\varepsilon\ \psi^\varepsilon \\ &= -\frac{\varepsilon^2}{2}\Delta\psi^\varepsilon + (V_0(\mathbf{x}) + W^\varepsilon(\mathbf{x}))\psi^\varepsilon + |\psi^\varepsilon|^2\psi^\varepsilon,\ \mathbf{x} \in \mathbb{R}^d, \quad (2.26) \end{aligned}$$

where $W^\varepsilon(\mathbf{x}) = \varepsilon^{2\alpha/(2+\alpha)}W(\mathbf{x}/\varepsilon^{2/(2+\alpha)})$ and the energy functional $E^\varepsilon(\psi^\varepsilon)$ is defined as

$$E^\varepsilon(\psi^\varepsilon) = \int_{\mathbb{R}^3}\left[\frac{\varepsilon^2}{2}|\nabla\psi^\varepsilon|^2 + (V_0(\mathbf{x}) + W^\varepsilon(\mathbf{x}))|\psi^\varepsilon|^2 + \frac{1}{2}|\psi^\varepsilon|^4\right]d\mathbf{x} = O(1).$$

Similarly, the nonlinear eigenvalue problem (2.20) (under the normalization (2.22) with $\phi = \phi^\varepsilon$) reads

$$\mu^\varepsilon\phi^\varepsilon(\mathbf{x}) = -\frac{\varepsilon^2}{2}\Delta\phi^\varepsilon + (V_0(\mathbf{x}) + W^\varepsilon(\mathbf{x}))\phi^\varepsilon + |\phi^\varepsilon|^2\phi^\varepsilon, \quad \mathbf{x} \in \mathbb{R}^d, \qquad (2.27)$$

where any eigenvalue μ^ε can be computed from its corresponding eigenfunction ϕ^ε by

$$\mu^\varepsilon = \mu^\varepsilon(\phi^\varepsilon) = \int_{\mathbb{R}^d}\left[\frac{\varepsilon^2}{2}|\nabla\phi^\varepsilon|^2 + (V_0(\mathbf{x}) + W^\varepsilon(\mathbf{x}))|\phi^\varepsilon|^2 + |\phi^\varepsilon|^4\right]d\mathbf{x} = O(1).$$

Furthermore it is easy to get the leading asymptotics of the energy functional $E(\psi)$ in (2.16) and the chemical potential (2.23) when $\beta_d \gg 1$ from this scaling:

$$E(\psi) = \varepsilon^{-2\alpha/(2+\alpha)}E^\varepsilon(\psi^\varepsilon) = O\left(\varepsilon^{-2\alpha/(2+\alpha)}\right) = O\left(\beta_d^{\alpha/(d+\alpha)}\right), \quad (2.28)$$

$$\mu(\phi) = \varepsilon^{-2\alpha/(2+\alpha)}\mu^\varepsilon(\phi^\varepsilon) = O\left(\varepsilon^{-2\alpha/(2+\alpha)}\right) = O\left(\beta_d^{\alpha/(d+\alpha)}\right). \quad (2.29)$$

In [17, 43], a different rescaling for the nonlinear schrödinger equation subject to smooth, lattice-periodic potentials was used in the semiclassical regime. There they studied Bloch waves dynamics in BEC on optical lattices.

3. Approximations in a Box Potential

In this section, we will present asymptotic approximations for the ground

and excited states, as well as their energy and chemical potential approximations up to $o(1)$ in term of β_d, in BEC with a box potential, i.e. $V_d(\mathbf{x}) \equiv 0$ and $\Omega = [0,1]^d$ in (2.20), in weakly interacting regime, i.e. $\beta_d \to 0$, and strongly repulsive interacting regime, i.e. $\beta_d \to \infty$, respectively. In this case, we have the following equalities between the energies and chemical potential:

$$E_{\rm int}(\phi) = \frac{1}{2}\left[\mu(\phi) - E_{\rm kin}(\phi)\right], \qquad E(\phi) = E_{\rm kin}(\phi) + E_{\rm int}(\phi). \tag{3.1}$$

3.1. Approximations in weakly interacting regime

When $\beta_d = 0$, the problem (2.20)-(2.22) reduces to a linear eigenvalue problem, i.e.

$$\mu\, \phi(\mathbf{x}) = -\frac{1}{2}\Delta\phi(\mathbf{x}), \quad \mathbf{x} \in \Omega, \qquad \phi(\mathbf{x})|_\Gamma = 0, \qquad \|\phi\| = 1. \tag{3.2}$$

By separation of variables, we can find a complete set of orthonormal eigenfunctions:

$$\phi_{\mathbf{J}}(\mathbf{x}) = \prod_{m=1}^{d} \phi_{j_m}(x_m),\ \phi_l(\tau) = \sqrt{2}\sin(l\pi\tau),\ l \in \mathbb{N},\ \mathbf{J} = (j_1, \ldots, j_d) \in \mathbb{N}^d. \tag{3.3}$$

The corresponding eigenvalues are

$$\mu_{\mathbf{J}} = \sum_{m=1}^{d} \mu_{j_m}, \qquad \mu_l = \frac{1}{2} l^2 \pi^2, \qquad l \in \mathbb{N}. \tag{3.4}$$

From these solutions, we can get the ground state solution $\phi_g(\mathbf{x}) = \phi_{(1,\ldots,1)}(\mathbf{x})$. The corresponding energy and chemical potential $E_g = \mu_g = d\pi^2/2$. All other eigenfunctions are excited states. Of course, these solutions can be viewed as approximations for the ground and excited states when $\beta_d = o(1)$ in (2.20) by dropping the nonlinear term on the right hand side of (2.20).

3.2. Thomas-Fermi (semiclassical) approximation

For strong repulsive interacting regime, i.e, $\beta_d \gg 1$, we can drop the diffusion term, i.e. the first term on the right hand side of (2.20) and get

$$\mu_g^{\rm TF}\ \phi_g^{\rm TF}(\mathbf{x}) = \beta_d\ \left|\phi_g^{\rm TF}(\mathbf{x})\right|^2 \phi_g^{\rm TF}(\mathbf{x}), \qquad \mathbf{x} \in \Omega. \tag{3.5}$$

From (3.5), we obtain

$$\phi_g^{\mathrm{TF}}(\mathbf{x}) = \sqrt{\frac{\mu_g^{\mathrm{TF}}}{\beta_d}}, \qquad \mathbf{x} \in \Omega. \tag{3.6}$$

Plugging (3.6) into the normalization condition (2.22), we obtain

$$1 = \int_\Omega |\phi_g^{\mathrm{TF}}(\mathbf{x})|^2 \, d\mathbf{x} = \int_\Omega \frac{\mu_g^{\mathrm{TF}}}{\beta_d} \, d\mathbf{x} = \frac{\mu_g^{\mathrm{TF}}}{\beta_d} \quad \Rightarrow \quad \mu_g^{\mathrm{TF}} = \beta_d. \tag{3.7}$$

Noticing (2.23), we get

$$E_g^{\mathrm{TF}} = \mu_g^{\mathrm{TF}} - \frac{\beta_d}{2} \int_\Omega |\phi_g^{\mathrm{TF}}|^4 \, d\mathbf{x} = \frac{\mu_g^{\mathrm{TF}}}{2} = \frac{\beta_d}{2}. \tag{3.8}$$

Therefore, we get the TF approximation for the ground state, the energy and the chemical potential when $\beta_d \gg 1$:

$$\phi_g(\mathbf{x}) \approx \phi_g^{\mathrm{TF}}(\mathbf{x}) = 1, \qquad \mathbf{x} \in \Omega, \tag{3.9}$$

$$E_g \approx E_g^{\mathrm{TF}} = \frac{\beta_d}{2}, \qquad \mu_g \approx \mu_g^{\mathrm{TF}} = \beta_d. \tag{3.10}$$

It is easy to see that the TF approximation for the ground state does not satisfy the boundary condition (2.21). This is due to removing the diffusion term in (2.20) and it suggests that a boundary layer will appear in the ground state when $\beta_d \gg 1$. Due to the existence of the boundary layer, the kinetic energy does not go to zero when $\beta_d \to \infty$ and thus it cannot be neglected. In the next subsection, we will present a better approximation by applying the matched asymptotic method.

3.3. Approximate ground state in 1D

When $d = 1$, $V_d(\mathbf{x}) \equiv 0$ and $\Omega = [0, 1]$ in (2.20), since the layers exist at two boundaries $x = 0$ and $x = 1$, we will solve (2.20) near $x = 0$ and $x = 1$, respectively. Firstly, we consider $0 \le x \le 1/2$ and rescale (2.20) by introducing

$$x = \frac{1}{\sqrt{\mu_g}} X, \qquad \phi(x) = \sqrt{\frac{\mu_g}{\beta_1}} \Phi(X), \tag{3.11}$$

where $\mu_g \approx \beta_1$ is the chemical potential of the ground state. Plugging (3.11)

into (2.20), a computation shows

$$\Phi(X) = -\frac{1}{2}\Phi_{XX}(X) + \Phi^3(X), \qquad 0 \le X < \infty, \tag{3.12}$$

$$\Phi(0) = 0, \qquad \lim_{X\to\infty} \Phi(X) = 1. \tag{3.13}$$

Solving (3.12)-(3.13), we obtain

$$\Phi(X) = \tanh\left(X\right), \qquad 0 \le X < \infty. \tag{3.14}$$

Plugging (3.14) into (3.11), we obtain an approximation for $\phi_g(x)$ near $x = 0$ when $\beta_1 \gg 1$:

$$\phi_g(x) \approx \sqrt{\frac{\mu_g}{\beta_1}} \tanh\left(\sqrt{\mu_g} x\right), \qquad 0 \le x < 1/2. \tag{3.15}$$

Similarly, we can get an approximation for $\phi_g(x)$ near $x = 1$ when $\beta_1 \gg 1$:

$$\phi_g(x) \approx \sqrt{\frac{\mu_g}{\beta_1}} \tanh\left(\sqrt{\mu_g}(1-x)\right), \qquad 1/2 < x \le 1. \tag{3.16}$$

From (3.15) and (3.16), noticing the boundary condition (2.21) and using the matched asymptotic method, we get an approximation for the ground state when $\beta_1 \gg 1$:

$$\begin{aligned}\phi_g(x) &\approx \phi_g^{\mathrm{MA}}(x) \\ &= \sqrt{\frac{\mu_g^{\mathrm{MA}}}{\beta_1}} \left[\tanh\left(\sqrt{\mu_g^{\mathrm{MA}}} x\right) + \tanh\left(\sqrt{\mu_g^{\mathrm{MA}}}(1-x)\right) - \tanh\left(\sqrt{\mu_g^{\mathrm{MA}}}\right)\right].\end{aligned} \tag{3.17}$$

Substituting (3.17) into (2.22), after some computations (see Appendix A1), we obtain

$$1 = \int_0^1 |\phi_g^{\mathrm{MA}}(x)|^2 \, dx \approx \frac{\mu_g^{\mathrm{MA}}}{\beta_1} - 2\frac{\sqrt{\mu_g^{\mathrm{MA}}}}{\beta_1}. \tag{3.18}$$

Solving (3.18), we get

$$\mu_g \approx \mu_g^{\mathrm{MA}} = \beta_1 + 2\sqrt{\beta_1 + 1} + 2 = \mu_g^{\mathrm{TF}} + 2\sqrt{\beta_1 + 1} + 2, \qquad \beta_1 \gg 1. \tag{3.19}$$

Plugging (3.17) into (2.17)-(2.18), after some computations (see Appendix A1), we obtain

$$E_{\mathrm{kin},g} \approx E_{\mathrm{kin},g}^{\mathrm{MA}} = \frac{2}{3}\sqrt{\beta_1 + 1} + 2, \tag{3.20}$$

$$E_{\mathrm{int},g} \approx E_{\mathrm{int},g}^{\mathrm{MA}} = \frac{\beta_1}{2} + \frac{2}{3}\sqrt{\beta_1 + 1}, \qquad \beta_1 \gg 1, \tag{3.21}$$

$$E_g \approx E_g^{\mathrm{MA}} = \frac{\beta_1}{2} + \frac{4}{3}\sqrt{\beta_1 + 1} + 2. \tag{3.22}$$

From the above asymptotic results, we can draw the following conclusions:

(i) The width of the boundary layer in the matched asymptotic approximation is about $O(1/\sqrt{\beta_1})$ from (3.17) and (3.19).

(ii) The ratios between the energies satisfy:

$$\lim_{\beta_1\to\infty} \frac{E_g}{\mu_g} = \frac{1}{2}, \quad \lim_{\beta_1\to\infty} \frac{E_{\mathrm{int},g}}{E_g} = 1, \quad \lim_{\beta_1\to\infty} \frac{E_{\mathrm{kin},g}}{E_g} = 0. \tag{3.23}$$

To verify (3.17), (3.20), (3.21), (3.22), (3.23) and (3.19) numerically, Table 1 lists the errors between the ground state and its matched asymptotic approximation, and Figure 1a shows the ground state for different β_1. In this table and the following, the convergence rate of a function $f(\alpha)$ as $\alpha \to 0$ is computed as: $\ln[f(2\alpha)/f(\alpha)]/\ln 2$.

Table 1. Convergence study of the matched asymptotic approximation for the ground state with 1D box potential when $\beta_1 \gg 1$.

$1/\beta_1$	4/25	2/25	1/25	1/50	1/100	1/400
$\max\lvert\phi_g - \phi_g^{\mathrm{MA}}\rvert$	8.17E-3	9.24E-4	4.67E-5	8E-7	– –	– –
$\lVert\phi_g - \phi_g^{\mathrm{MA}}\rVert_{L^2}$	6.84E-3	8.05E-4	4.11E-5	6E-7	– –	– –
$\lvert E_{\mathrm{kin},g} - E_{\mathrm{kin},g}^{\mathrm{MA}}\rvert$	1.3018	0.9479	0.6464	0.4340	0.2946	0.1399
Rate		0.4577	0.5523	0.5747	0.5589	0.5372
$\lvert E_{\mathrm{int},g} - E_{\mathrm{int,g}}^{\mathrm{MA}}\rvert$	0.5948	0.4608	0.3218	0.2171	0.1473	0.0701
Rate		0.3683	0.5180	0.5678	0.5596	0.5356
$\lvert E_g - E_g^{\mathrm{MA}}\rvert$	0.7071	0.4871	0.3245	0.2171	0.1472	0.0698
Rate		0.5377	0.5860	0.5799	0.5606	0.5382
$\lvert\mu_g - \mu_g^{\mathrm{MA}}\rvert$	0.1124	0.0263	0.0027	0.0001	– –	– –
E_g/μ_g	0.6854	0.6234	0.5813	0.5543	0.5368	0.5175
$E_{\mathrm{int},g}/E_g$	0.4591	0.6042	0.7204	0.8042	0.8628	0.9323
$E_{\mathrm{kin},g}/E_g$	0.5409	0.3958	0.2796	0.1958	0.1372	0.0677

From Table 1 and Figure 1a, we can draw the following conclusions:

(1) The matched asymptotic approximation converges to the ground

state, when $\beta_1 \to \infty$, with the convergence rate

$$\max|\phi_g - \phi_g^{\rm MA}| = O(e^{-3\sqrt{\beta_1}/2}),\ \|\phi_g - \phi_g^{\rm MA}\|_{L^2} = O(e^{-3\sqrt{\beta_1}/2}),\ \beta_1 \gg 1.$$

(2) The asymptotic approximations (3.19)-(3.23) are confirmed. Furthermore our numerical results suggest the following convergence rate

$$E_{{\rm kin},g} = E_{{\rm kin},g}^{\rm MA} + O(1/\sqrt{\beta_1}), \quad E_{{\rm int},g} = E_{{\rm int},g}^{\rm MA} + O(1/\sqrt{\beta_1}),$$
$$E_g = E_g^{\rm MA} + O(1/\sqrt{\beta_1}),\ \mu_g = \mu_g^{\rm MA} + O(e^{-3\sqrt{\beta_1}/2}), \quad \beta_1 \gg 1.$$

(3) Boundary layers are observed at $x = 0$ and $x = 1$ in the ground state when $\beta_1 \gg 1$ and the width of the layers is about $2/\sqrt{\beta_1}$. Here the width of the layer is measured numerically from the wave function changing from 0 to 0.7.

3.4. Approximate excited states in 1D

Similar as the procedure used in the previous subsection for ground state, here we construct matched asymptotic approximations for the excited states in 1D in the semiclassical regime. In fact, when $\beta_1 \gg 1$, the kth ($k \in \mathbb{N}$) excited state has two boundary layers located at $x = 0$ and $x = 1$ and k interior layers located at $x = j/(k+1)$ ($j = 1, \ldots, k$). Using the matched asymptotic method, we can obtain an approximation $\phi_k^{\rm MA}(x)$ for the kth excited states ϕ_k ($k \in \mathbb{N}$) as:

$$\phi_k(x) \approx \phi_k^{\rm MA}(x) = \sqrt{\frac{\mu_k^{\rm MA}}{\beta_1}}\left[\sum_{j=0}^{[(k+1)/2]} \tanh\left(\sqrt{\mu_k^{\rm MA}}\left(x - \frac{2j}{k+1}\right)\right)\right.$$
$$\left. + \sum_{j=0}^{[k/2]} \tanh\left(\sqrt{\mu_k^{\rm MA}}\left(\frac{2j+1}{k+1} - x\right)\right) - C_k \tanh\left(\sqrt{\mu_k^{\rm MA}}\right)\right],\ k \in \mathbb{N}, \quad (3.24)$$

where $[\tau]$ takes the integer part of the real number τ and the constant C_k is chosen as

$$C_k = \begin{cases} 1, & k \text{ even}, \\ 0, & k \text{ odd}, \end{cases} \qquad n \in \mathbb{N}.$$

Substituting (3.24) into (2.22), after some computations (see Appendix A2),

we obtain

$$1 = \int_0^1 |\phi_k^{\mathrm{MA}}(x)|^2 \, dx \approx \frac{\mu_k^{\mathrm{MA}}}{\beta_1} \left[1 - \frac{2(k+1)}{\sqrt{\mu_k^{\mathrm{MA}}}} \right]. \tag{3.25}$$

Solving (3.25), we obtain an approximation for the chemical potential of the kth excited state

$$\mu_k \approx \mu_k^{\mathrm{MA}} = \beta_1 + 2(k+1)\sqrt{\beta_1 + (k+1)^2} + 2(k+1)^2, \quad k \in \mathbb{N}. \tag{3.26}$$

Plugging (3.24) into (2.17)-(2.18), after some computations (see Appendix A2), we get

$$E_{\mathrm{kin},k} \approx E_{\mathrm{kin},k}^{\mathrm{MA}} = \frac{2}{3}(k+1)\sqrt{\beta_1 + (k+1)^2} + 2(k+1)^2, \tag{3.27}$$

$$E_{\mathrm{int,k}} \approx E_{\mathrm{int,k}}^{\mathrm{MA}} = \frac{\beta_1}{2} + \frac{2}{3}(k+1)\sqrt{\beta_1 + (k+1)^2}, \ k \in \mathbb{N}, \ \beta_1 \gg 1, \tag{3.28}$$

$$E_k \approx E_k^{\mathrm{MA}} = \frac{\beta_1}{2} + \frac{4}{3}(k+1)\sqrt{\beta_1 + (k+1)^2} + 2(k+1)^2. \tag{3.29}$$

From (3.26)-(3.29) and (3.19)-(3.22), we can formally draw the following conclusion when $\beta_1 \gg 1$:

If all the eigenfunctions, i.e. ϕ_g, ϕ_1, ϕ_2, $\cdots$, of the nonlinear eigenvalue problem (2.23) are ranked according to their energies, then the corresponding eigenvalues (or chemical potentials) are ranked in the same order, i.e.

$$E(\phi_g) < E(\phi_1) < E(\phi_2) < \cdots \quad \Longrightarrow \quad \mu(\phi_g) < \mu(\phi_1) < \mu(\phi_2) < \cdots. \tag{3.30}$$

This suggests that the two definitions of the ground state used in physics literatures, i.e. (1) minimizer of the minimization problem (2.24), (2) eigenfunction of the nonlinear eigenvalue problem (2.20) with smallest eigenvalue, are equivalent. Furthermore, we have

$$\lim_{\beta_1 \to \infty} \frac{E_k}{E_g} = 1, \qquad \lim_{\beta_1 \to \infty} \frac{\mu_k}{\mu_g} = 1, \qquad \lim_{\beta_1 \to \infty} \frac{E_k}{\mu_g} = \frac{1}{2}, \tag{3.31}$$

$$\lim_{\beta_1 \to \infty} \frac{E_{\mathrm{int},k}}{E_k} = 1, \qquad \lim_{\beta_1 \to \infty} \frac{E_{\mathrm{kin},k}}{E_k} = 0, \qquad k \in \mathbb{N}. \tag{3.32}$$

Again, to verify the results (3.24),(3.26)-(3.32) numerically, Tables 2 and 3 list the errors between the 1st and 5th excited states and their matched

asymptotic approximations, respectively. Table 4 lists the energy and chemical potential of the ground state and first five excited states for different β_1. Furthermore, Figure 1b and c shows the 1st and 5th excited states for different β_1.

Table 2. Convergence study of the matched asymptotic approximation for the 1st excited state with 1D box potential when $\beta_1 \gg 1$.

$1/\beta_1$	1/25	1/50	1/100	1/400	1/1600	1/6400
$\max\|\phi_1 - \phi_1^{\rm MA}\|$	6.44E-3	7.12E-4	3.54E-5	– –	– –	– –
$\|\phi_1 - \phi_1^{\rm MA}\|_{L^2}$	5.28E-3	6.02E-4	2.99E-5	– –	– –	– –
$\|E_{\rm kin,1} - E_{\rm kin,1}^{\rm MA}\|$	5.2073	3.7918	2.5854	1.1783	0.5597	0.2700
Rate		0.4577	0.5525	0.5668	0.5370	0.5258
$\|E_{\rm int,1} - E_{\rm int,1}^{\rm MA}\|$	2.3788	1.8432	1.2874	0.5894	0.2804	0.1367
Rate		0.3680	0.5178	0.5636	0.5359	0.5182
$\|E_1 - E_1^{\rm MA}\|$	2.8285	1.9487	1.2981	0.5890	0.2794	0.1333
Rate		0.5375	0.5861	0.5700	0.5380	0.5338
$\|\mu_1 - \mu_1^{\rm MA}\|$	0.4496	0.1055	0.0106	0.0003	– –	– –
E_1/μ_1	0.6854	0.6241	0.5813	0.5368	0.5175	0.5085
$E_{\rm int,1}/E_1$	0.4591	0.6042	0.7204	0.8628	0.9323	0.9664
$E_{\rm kin,1}/E_1$	0.5409	0.3958	0.2796	0.1372	0.0677	0.0336

Table 3. Convergence study of the matched asymptotic approximation for the 5th excited state with 1D box potential when $\beta_1 \gg 1$.

$1/\beta_1$	1/50	1/100	1/400	1/1600	1/6400	1/12800
$\max\|\phi_5 - \phi_5^{\rm MA}\|$	0.1451	0.0437	0.0011	– –	– –	– –
$\|\phi_5 - \phi_5^{\rm MA}\|_{L^2}$	0.1072	0.0337	0.0009	– –	– –	– –
$\|E_{\rm kin,5} - E_{\rm kin,5}^{\rm MA}\|$	68.955	60.445	36.230	16.711	7.7560	5.3607
Rate		0.1900	0.3692	0.5582	0.5537	0.5329
$\|E_{\rm int,5} - E_{\rm int,5}^{\rm MA}\|$	25.409	24.679	17.477	8.3534	3.8800	2.6840
Rate		0.0421	0.2489	0.5325	0.5532	0.5317
$\|E_5 - E_5^{\rm MA}\|$	43.546	35.766	18.754	8.3580	3.8760	2.6766
Rate		0.2840	0.4657	0.5830	0.5543	0.5342
$\|\mu_5 - \mu_5^{\rm MA}\|$	18.137	11.087	1.2770	0.0046	0.0040	– –
E_5/μ_5	0.8541	0.7772	0.6325	0.5581	0.5269	0.5186
$E_{\rm int,5}/E_5$	0.1708	0.2867	0.5811	0.7919	0.8977	0.9281
$E_{\rm kin,5}/E_5$	0.8292	0.7133	0.4189	0.2081	0.1023	0.0719

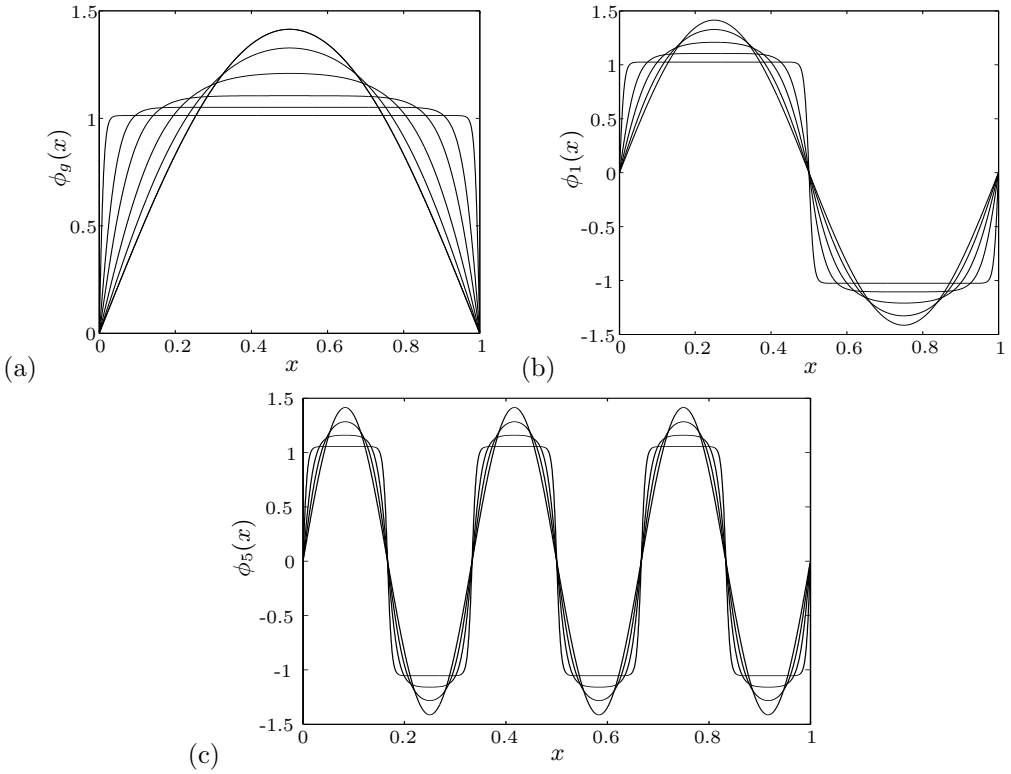

Figure 1. Ground and excited states with 1D box potential for increasing β_1 (in the order of decreasing peak). a). Ground state for $\beta_1 = 0, 6.25, 25, 100, 400, 6400$; b). 1st excited state for $\beta_1 = 0, 25, 100, 400, 6400$; c). 5th excited state for $\beta_1 = 0, 400, 1600, 12800$.

From Tables 2, 3 and 4 and Figure 1b and c, we can draw the following conclusions for the excited states:

(1) The conclusions (1) and (2) for the ground state in the previous subsection are still valid for the excited states.

(2) Boundary layers at $x = 0$ and $x = 1$ and interior layers at $x = j/(k+1)$ $(j = 1, \ldots, k)$ are observed in the kth excited state when $\beta_1 \gg 1$. The width of the boundary layers is about $2/\sqrt{\beta_1}$ and that of the interior layers is about $4/\sqrt{\beta_1}$.

(3) The conclusions (3.31), (3.32) and (3.30) are confirmed by our numerical results. In fact, (3.30) is valid for all $\beta_1 \geq 0$.

Furthermore, a by-product observation from our numerical simulation is that the CNGF and its BEFD discretization [6] can be used to compute ground and all excited states in box potential provided appropriate initial data is chosen. To compute the ground state, one can choose the initial data as $\phi_0(x) = \sqrt{2}\sin(\pi x)$, and for computing the kth excited state, one can choose initial data as $\phi_0(x) = \sqrt{2}\sin((k+1)\pi x)$. The reason that the algorithm can be used to compute any excited state is due to that the roots of any fixed kth excited state are independent of β_1. Extension of this observation to high dimension is straightforward by tensor product.

Table 4. Energy and chemical potential for the ground state and first five excited states with 1D box potential.

β_1	0	25	100	400	1600	6400	25600
E_g	4.9348	21.623	65.547	228.77	855.38	3308.7	13015
E_1	19.739	37.689	86.493	262.19	915.08	3421.5	13235
E_2	44.413	62.765	114.45	300.98	979.42	3538.7	13458
E_3	78.956	97.473	150.76	345.97	1048.8	3660.3	13686
E_4	123.37	141.97	196.17	397.99	1123.5	3786.6	13917
E_5	177.65	196.30	251.06	457.80	1203.9	3917.7	14153
μ_g	4.9348	37.201	122.10	442.05	1682.0	6562.0	25922
μ_1	19.739	54.990	148.80	488.40	1768.2	6728.1	26248
μ_2	44.413	80.758	180.96	539.34	1858.7	6898.3	26578
μ_3	78.956	151.77	219.96	595.21	1953.6	7072.8	26912
μ_4	123.37	160.42	267.06	656.48	2053.1	7251.6	27251
μ_5	177.65	214.83	323.03	723.84	2157.4	7434.7	27593

3.5. Extension to high dimensions

In this subsection, we extend the matched asymptotic approximation for the 1D ground state to high dimensions, i.e d-dimensions ($d > 1$). Similar to the 1D case, we can get the approximation for the ground state in d-dimensions with $\mathbf{x} = (x_1, \ldots, x_d)^T$:

$$\phi_g(\mathbf{x}) \approx \phi_g^{\mathrm{MA}}(\mathbf{x}) = \sqrt{\frac{\mu_g^{\mathrm{MA}}}{\beta_d}} \prod_{j=1}^{d} \left[\tanh\left(\sqrt{\mu_g^{\mathrm{MA}}} x_j\right) + \tanh\left(\sqrt{\mu_g^{\mathrm{MA}}}(1-x_j)\right) - \tanh\left(\sqrt{\mu_g^{\mathrm{MA}}}\right) \right]. \quad (3.33)$$

Plugging (3.33) into (2.22) and after a simple computation, we obtain

$$1 = \int_{(0,1)^d} |\phi_g^{\mathrm{MA}}(\mathbf{x})|^2 d\mathbf{x} \approx \frac{\mu_g^{\mathrm{MA}}}{\beta_d}\Big(1 - \frac{2}{\sqrt{\mu_g^{\mathrm{MA}}}}\Big)^d. \tag{3.34}$$

Solving (3.34), we get an approximation for the chemical potential when $\beta_d \gg 1$,

$$\mu_g \approx \mu_g^{\mathrm{MA}} = \beta_d + 2d\sqrt{\beta_d + d(2-d)} + 2d, \qquad d > 1. \tag{3.35}$$

Similarly, we can get approximations for different energies of the ground state:

$$E_{\mathrm{kin},g} \approx E_{\mathrm{kin},g}^{\mathrm{MA}} = \frac{2d}{3}\sqrt{\beta_d + d(2-d)} + \frac{2d}{3}(d+2), \tag{3.36}$$

$$E_{\mathrm{int},g} \approx E_{\mathrm{int},g}^{\mathrm{MA}} = \frac{\beta_d}{2} + \frac{2d}{3}\sqrt{\beta_d + d(2-d)} + \frac{1}{3}d(1-d), \quad d > 1, \tag{3.37}$$

$$E_g \approx E_g^{\mathrm{MA}} = \frac{\beta_d}{2} + \frac{4d}{3}\sqrt{\beta_d + d(2-d)} + \frac{1}{3}d(d+5). \tag{3.38}$$

4. Approximations in Nonuniform Potentials

In this section, we will find the energy and chemical potential asymptotics up to $o(1)$ in term of β_d in BEC with a nonuniform external potential, i.e. $V_d(\mathbf{x}) \neq 0$ and $\Omega = \mathbb{R}^d$ in (2.20), in the semiclassical regime. When $\beta_d \gg 1$, we can ignore the kinetic term in (2.20) and derive the TF approximation:

$$\mu_g^{\mathrm{TF}}\ \phi_g^{\mathrm{TF}}(\mathbf{x}) = V_d(\mathbf{x})\phi_g^{\mathrm{TF}}(\mathbf{x}) + \beta_d|\phi_g^{\mathrm{TF}}(\mathbf{x})|^2\phi_g^{\mathrm{TF}}(\mathbf{x}), \qquad \mathbf{x} \in \mathbb{R}^d. \tag{4.1}$$

Solving (4.1), we obtain the TF approximation for the ground state:

$$\phi_g^{\mathrm{TF}}(\mathbf{x}) = \begin{cases} \sqrt{\left(\mu_g^{\mathrm{TF}} - V_d(\mathbf{x})\right)/\beta_d}, & V_d(\mathbf{x}) \le \mu_g^{\mathrm{TF}}, \\ 0, & \text{otherwise}, \end{cases} \tag{4.2}$$

where μ_g^{TF} is determined from the normalization condition

$$\|\phi_g^{\mathrm{TF}}\|^2 := \int_{\mathbb{R}^d} |\phi_g^{\mathrm{TF}}(\mathbf{x})|^2\, d\mathbf{x} = 1. \tag{4.3}$$

Due to the fact $\phi_g^{\mathrm{TF}}(\mathbf{x})$ is not differentiable at $V_d(\mathbf{x}) = \mu_g^{\mathrm{TF}}$, as observed in

[8, 11, 12], $E(\phi_g^{\rm TF}) = \infty$ and $E_{\rm kin}(\phi_g^{\rm TF}) = \infty$, one cannot use the definition (2.16) and (2.18) to define the energy and kinetic energy of the TF approximation (4.2) respectively. Noticing (2.23) and (2.18), as proposed in [8, 11, 12], here we use the following way to calculate them:

$$E_g^{\rm TF} \approx E_g = E(\phi_g) = \mu(\phi_g) - E_{\rm int}(\phi_g) \approx \mu_g^{\rm TF} - E_{{\rm int},g}^{\rm TF}, \tag{4.4}$$

$$E_{{\rm kin},g}^{\rm TF} \approx E_{{\rm kin},g} = E(\phi_g) - E_{\rm int}(\phi_g) - E_{\rm pot}(\phi_g) \approx E_g^{\rm TF} - E_{{\rm int},g}^{\rm TF} - E_{{\rm pot},g}^{\rm TF}, \tag{4.5}$$

where

$$E_{{\rm int},g}^{\rm TF} = E_{\rm int}(\phi_g^{\rm TF}), \qquad E_{{\rm pot},g}^{\rm TF} = E_{\rm pot}(\phi_g^{\rm TF}).$$

4.1. Approximation in a harmonic oscillator potential

For 1D BEC with a harmonic oscillator potential, we choose $d = 1$ and $V_1(x) = \gamma_x^2 x^2/2$ with $\gamma_x > 0$ in (4.2). Then plugging (4.2) into (4.3), after a detailed computation (see Appendix B1), we obtain

$$1 = \int_{-\infty}^{\infty} |\phi_g^{\rm TF}|^2 \, dx = \frac{2}{3} \frac{\left(2\mu_g^{TF}\right)^{3/2}}{\beta_1 \gamma_x}. \tag{4.6}$$

Solving (4.6), we obtain the chemical potential asymptotics when $\beta_1 \gg 1$

$$\mu_g \approx \mu_g^{\rm TF} = \frac{1}{2} \left(\frac{3\beta_1 \gamma_x}{2} \right)^{2/3}. \tag{4.7}$$

Substituting (4.2) in this case into (2.17), after some computations (see Appendix B1), we obtain

$$E_{{\rm int},g} \approx E_{{\rm int},g}^{\rm TF} = \frac{1}{5} \left(\frac{3\beta\gamma_x}{2} \right)^{2/3}, \quad E_{{\rm pot},g} \approx E_{\rm pot,g}^{\rm TF} = \frac{1}{10} \left(\frac{3\beta\gamma_x}{2} \right)^{2/3}, \tag{4.8}$$

$$E_g \approx E_g^{\rm TF} = \frac{3}{10} \left(\frac{3\beta\gamma_x}{2} \right)^{2/3}, \quad E_{{\rm kin},g} \approx E_{{\rm kin},g}^{\rm TF} = 0. \tag{4.9}$$

From (4.7), (4.8) and (4.9), we obtain

$$\lim_{\beta_1 \to \infty} \frac{E_g}{\mu_g} = \frac{3}{5}, \qquad \lim_{\beta_1 \to \infty} \frac{E_{{\rm int},g}}{E_g} = \frac{2}{3}, \qquad \lim_{\beta_1 \to \infty} \frac{E_{{\rm pot},g}}{E_g} = \frac{1}{3}. \tag{4.10}$$

To verify the TF approximation (4.2) in this case and (4.7)-(4.10) numerically, Table 5 lists the errors between the ground state and its TF approx-

imation, and Table 6 lists the energy and chemical potential of the ground and first excited states. Furthermore, Figure 2 shows the ground and first excited states for different β_1.

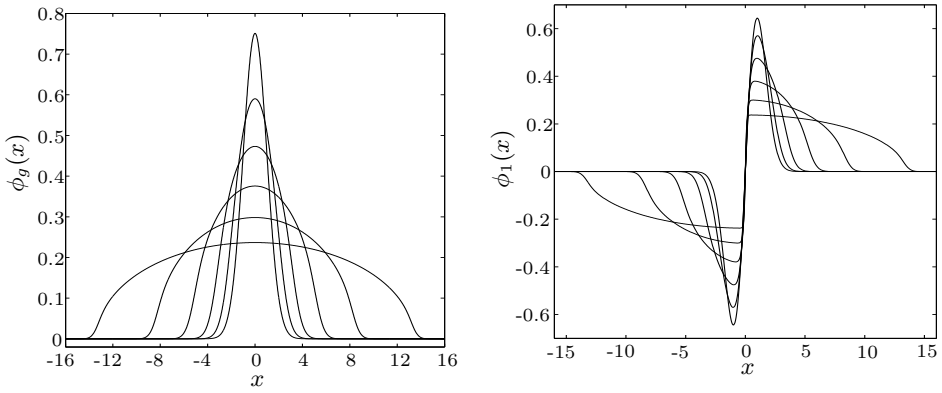

Figure 2. Ground (left) and first excited (right) states with 1D harmonic oscillator potential $V_1(x) = x^2/2$ for $\beta_1 = 0, 6.25, 25, 100, 400, 1600$ (in the order of decreasing peaks).

From Tables 5 and 6 and Figure 2, we can draw the following conclusions:

(1). The TF approximation converges to the ground state, when $\beta_1 \to \infty$, with the convergence rate $\theta_1 = 2/5$

$$\max|\phi_g - \phi_g^{\rm TF}| = O\left(\frac{\ln\beta_1}{\beta_1^{\theta_1}}\right), \qquad \|\phi_g - \phi_g^{\rm TF}\|_{L^2} = O\left(\frac{\ln\beta_1}{\beta_1^{\theta_1}}\right).$$

(2) The TF approximation (4.2) in this case and (4.7)-(4.10) are confirmed. Furthermore our numerical results suggest the following convergence rate $\theta_2 = 2/3$

$$E_{{\rm kin},g} = O\left(\frac{\ln\beta_1}{\beta_1^{\theta_2}}\right),\ E_{{\rm int},g} = E_{{\rm int},g}^{\rm TF} + O\left(\frac{\ln\beta_1}{\beta_1^{\theta_2}}\right),$$
$$E_{{\rm pot},g} = E_{{\rm pot},g}^{\rm TF} + O\left(\frac{\ln\beta_1}{\beta_1^{\theta_2}}\right),\ E_g = E_g^{\rm TF} + O\left(\frac{\ln\beta_1}{\beta_1^{\theta_2}}\right),$$
$$\mu_g = \mu_g^{\rm TF} + O\left(\frac{\ln\beta_1}{\beta_1^{\theta_2}}\right), \qquad \beta_1 \gg 1.$$

(3) Interior layer is observed at $x = 0$ in the first excited state when $\beta_1 \gg 1$ and the width of the layer is about $O(1/\beta_1^{1/3})$.

(4) The energy and chemical potential of the ground and first excited states are in the same order for any $\beta_1 \geq 0$, i.e.

$$E(\phi_g) < E(\phi_1) \quad \Longrightarrow \quad \mu(\phi_g) < \mu(\phi_1).$$

Table 5. Convergence study for the TF approximation with 1D harmonic oscillator potential $V_1(x) = x^2/2$.

$1/\beta_1$	1/100	1/200	1/400	1/800	1/1600	1/6400
$\max \lvert\phi_g - \phi_g^{\rm TF}\rvert$	0.0788	0.0605	0.0464	0.0355	0.0272	0.0159
Rate		0.3807	0.3836	0.3840	0.3852	0.3872
$\lVert\phi_g - \phi_g^{\rm TF}\rVert_{L^2}$	0.0571	0.04230	0.0312	0.0230	0.0170	0.0092
Rate		0.4350	0.4371	0.4389	0.4404	0.4427
$\lvert E_{{\rm pot},g} - E_{{\rm pot},g}^{\rm TF}\rvert$	0.0246	0.0171	0.0118	0.0080	0.0054	0.0023
Rate		0.5238	0.5383	0.5528	0.5687	0.6196
$\lvert E_{{\rm int},g} - E_{{\rm int},g}^{\rm TF}\rvert$	0.0204	0.0144	0.0101	0.0070	0.0047	0.0021
Rate		0.4980	0.5167	0.5348	0.5531	0.6051
$E_{{\rm kin},g} - 0$	0.0350	0.0245	0.0170	0.0117	0.0080	0.0037
Rate		0.5134	0.5267	0.5381	0.5478	0.5599
$\lvert E_g - E_g^{\rm TF}\rvert$	0.0392	0.0272	0.0187	0.0128	0.0087	0.0039
Rate		0.5280	0.5394	0.5492	0.5582	0.5725
$\lvert\mu_g - \mu_g^{\rm TF}\rvert$	0.0188	0.0128	0.0086	0.0058	0.0039	0.0019
Rate		0.5613	0.5651	0.5659	0.5638	0.5329
E_g/μ_g	0.6020	0.6009	0.6004	0.6002	0.6001	0.6000
$E_{{\rm int},g}/E_g$	0.6612	0.6643	0.6656	0.6662	0.6665	0.6666
$E_{{\rm pot},g}/E_g$	0.3347	0.3339	0.3336	0.3334	0.3334	0.3333

Table 6. Energy and chemical potential of the ground and first excited states with 1D harmonic oscillator potential $V_1(x) = x^2/2$.

β_1	0	25	100	400	1600	6400	25600
E_g	0.5000	3.4402	8.5085	21.360	55.786	135.51	341.46
E_1	1.5000	4.2115	9.2419	22.078	54.497	136.22	342.17
μ_g	0.5000	5.6421	14.134	35.578	89.632	225.85	569.10
μ_1	1.5000	6.3732	14.850	36.288	90.340	226.56	569.80

4.2. Approximation in a double-well potential

For 1D BEC with a double well potential, we choose $d = 1$ and $V_1(x) = \gamma_x^4(x^2 - a^2)^2/2$ with $\gamma_x > 0$ and $a \geq 0$, in (4.2). Then plugging (4.2) into (4.3), after a detailed computation (see Appendix B2), we obtain

$$\begin{aligned} 1 &= \int_{-\infty}^{\infty} |\phi_g^{\mathrm{TF}}(x)|^2 \, dx \\ &= \frac{4}{15\beta_1\gamma_x}\left(6\mu_g^{\mathrm{TF}} + a^2\gamma_x^2\sqrt{2\mu_g^{\mathrm{TF}}} - 2a^4\gamma_x^4\right)\sqrt{\sqrt{2\mu_g^{\mathrm{TF}}} + a^2\gamma_x^2}. \quad (4.11) \end{aligned}$$

Solving (4.11), we get the TF approximation for the chemical potential

$$\mu_g \approx \mu_g^{\mathrm{TF}} = \frac{1}{8}(50\beta_1^2\gamma_x^2)^{2/5} - \frac{a^2\gamma_x^2}{6}(50\beta_1^2\gamma_x^2)^{1/5} + \frac{7a^4\gamma_x^4}{18}. \quad (4.12)$$

Plugging(4.2) in this case into (2.17), after some computations (see Appendix B2), we get

$$E_{\mathrm{int},g} \approx E_{\mathrm{int},g}^{\mathrm{TF}} = \frac{1}{18}\left(50\beta_1^2\gamma_x^2\right)^{2/5} - \frac{a^2\gamma_x^2}{21}\left(50\beta_1^2\gamma_x^2\right)^{1/5}, \quad (4.13)$$

$$E_{\mathrm{pot},g} \approx E_{\mathrm{pot},g}^{\mathrm{TF}} = \frac{1}{72}\left(50\beta_1^2\gamma_x^2\right)^{2/5} - \frac{a^2\gamma_x^2}{14}\left(50\beta_1^2\gamma_x^2\right)^{1/5} + \frac{7a^4\gamma_x^4}{18}, \quad (4.14)$$

$$E_g \approx E_g^{\mathrm{TF}} = \frac{5}{72}\left(50\beta_1^2\gamma_x^2\right)^{2/5} - \frac{5}{42}a^2\gamma_x^2\left(50\beta_1^2\gamma_x^2\right)^{1/5} + \frac{7a^4\gamma_x^4}{18}, \quad (4.15)$$

$$E_{\mathrm{kin},g} \approx E_{\mathrm{kin},g}^{\mathrm{TF}} = 0. \quad (4.16)$$

From (4.12), (4.13), (4.14) and (4.15), we obtain

$$\lim_{\beta_1\to\infty}\frac{E_g}{\mu_g} = \frac{5}{9}, \qquad \lim_{\beta_1\to\infty}\frac{E_{\mathrm{int},g}}{E_g} = \frac{4}{5}, \qquad \lim_{\beta_1\to\infty}\frac{E_{\mathrm{pot},g}}{E_g} = \frac{1}{5}. \quad (4.17)$$

To verify (4.2) in this case and (4.12)-(4.17) numerically, Table 7 lists the errors between the ground state and its TF approximation and Table 8 lists the energy and chemical potential of the ground and first excited states when we choose $d = 1$ and $V_1(x) = (x^2 - 3^2)^2/2$ in (2.20). Furthermore, Figure 3 shows the ground and first excited state for different β_1.

From Tables 7 and 8 and Figure 3, the conclusions (1)-(4) in §4.1 are still valid except that we need to replace θ_1, θ_2 by $\theta_1 = 2/5$, $\theta_2 = 2/5$ and the width of the interior layers by $O(1/\beta_1^{2/5})$.

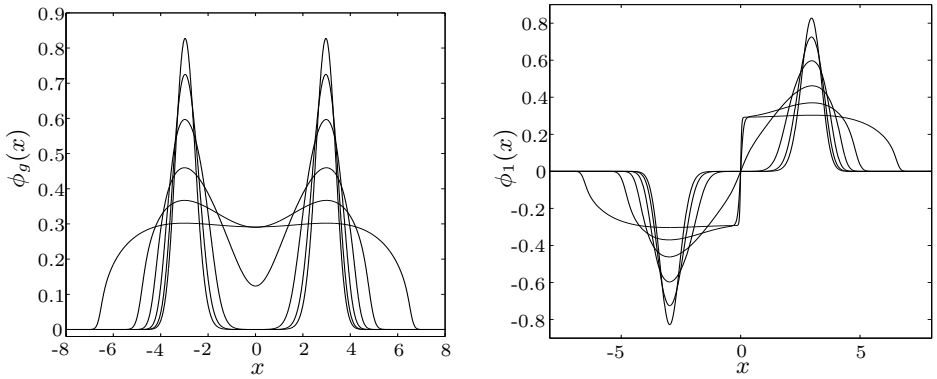

Figure 3. Ground (left) and first excited (right) states with a type I double-well potential $V_1(x) = (x^2 - 3^2)/2$ for $\beta_1 = 0, 12.5, 50, 200, 800, 6400$ (in the order of decreasing peaks).

Table 7. Convergence study of the TF approximation with a type I double-well potential $V_1(x) = (x^2 - 3^2)^2/2$.

$1/\beta_1$	1/100	1/400	1/1600	1/6400	1/25600	1/51200
$\max\lvert\phi_g - \phi_g^{\rm TF}\rvert$	0.1260	0.0915	0.0634	0.0429	0.0286	0.0233
Rate		0.2312	0.2638	0.2824	0.2921	0.2950
$\lVert\phi_g - \phi_g^{\rm TF}\rVert_{L^2}$	0.2238	0.0495	0.0254	0.0149	0.0087	0.0066
Rate		1.0888	0.4806	0.3865	0.3892	0.3958
$\lvert E_{{\rm pot},g} - E_{{\rm pot},g}^{\rm TF}\rvert$	18.824	8.7812	4.0019	2.0167	1.0758	0.7963
Rate		0.5500	0.5669	0.4943	0.4533	0.4340
$\lvert E_{{\rm int},g} - E_{{\rm int},g}^{\rm TF}\rvert$	6.0436	3.1554	1.3089	0.6176	0.3157	0.2303
Rate		0.4688	0.6347	0.5418	0.4841	0.4550
$E_{{\rm kin},g} - 0$	0.3982	0.1460	0.0854	0.0565	0.0376	0.0306
Rate		0.7238	0.3868	0.2980	0.2938	0.2972
$\lvert E_g - E_g^{\rm TF}\rvert$	12.382	5.4797	2.6076	1.3426	0.7225	0.5355
Rate		0.5880	0.5357	0.4788	0.4470	0.4321
$\lvert\mu_g - \mu_g^{\rm TF}\rvert$	6.3386	2.3244	1.2986	0.7249	0.4067	0.3051
Rate		0.7237	0.4180	0.4206	0.4169	0.4147
E_g/μ_g	0.6212	0.6182	0.5671	0.5482	0.5465	0.5476
$E_{{\rm int},g}/E_g$	0.6099	0.6175	0.7632	0.8240	0.8297	0.8263
$E_{{\rm pot},g}/E_g$	0.3674	0.3789	0.2359	0.1758	0.1703	0.1737

Table 8. Energy and chemical potential of the ground and first excited states with a type I double-well potential $V_1(x) = (x^2 - 3^2)^2/2$.

β_1	0	25	100	400	1600	3200	25600
E_g	2.9716	7.8639	17.555	40.357	105.56	320.41	1011.3
E_1	2.9716	7.8639	17.555	40.790	107.05	323.06	1015.3
μ_g	2.9716	11.990	28.261	65.277	186.14	584.43	1850.4
μ_1	2.9716	11.990	28.261	66.396	188.42	587.99	1855.5

Remark 4.1. In physics literatures [16, 30], another type double well potential, i.e. $d = 1$ and $V_1(x) = \gamma_x^2(|x| - a)^2/2$ with $\gamma_x > 0$ and $a \geq 0$ in (2.12) is also used. Similarly, for this case, we have

$$\mu_g \approx \mu_g^{\mathrm{TF}} = \frac{1}{2}\left(\frac{3\beta_1\gamma_x}{2}\right)^{2/3} - \frac{a\gamma_x}{2}\left(\frac{3\beta_1\gamma_x}{2}\right)^{1/3} + \frac{3}{8}a^2\gamma_x^2, \tag{4.18}$$

$$E_{\mathrm{int},g} \approx E_{\mathrm{int},g}^{\mathrm{TF}} = \frac{1}{5}\left(\frac{3\beta_1\gamma_x}{2}\right)^{2/3} - \frac{a\gamma_x}{8}\left(\frac{3\beta_1\gamma_x}{2}\right)^{1/3}, \tag{4.19}$$

$$E_{\mathrm{pot},g} \approx E_{\mathrm{pot},g}^{\mathrm{TF}} = \frac{1}{10}\left(\frac{3\beta_1\gamma_x}{2}\right)^{2/3} - \frac{a\gamma_x}{4}\left(\frac{3\beta_1\gamma_x}{2}\right)^{1/3} + \frac{3}{8}a^2\gamma_x^2, \tag{4.20}$$

$$E_g \approx E_g^{\mathrm{TF}} = \frac{3}{10}\left(\frac{3\beta_1\gamma_x}{2}\right)^{2/3} - \frac{3a\gamma_x}{8}\left(\frac{3\beta_1\gamma_x}{2}\right)^{1/3} + \frac{3}{8}a^2\gamma_x^2, \tag{4.21}$$

$$E_{\mathrm{kin},g} \approx E_{\mathrm{kin},g}^{\mathrm{TF}} = 0, \tag{4.22}$$

$$\lim_{\beta_1\to\infty}\frac{E_g}{\mu_g} = \frac{3}{5}, \qquad \lim_{\beta_1\to\infty}\frac{E_{\mathrm{int},g}}{E_g} = \frac{2}{3}, \qquad \lim_{\beta_1\to\infty}\frac{E_{\mathrm{pot},g}}{E_g} = \frac{1}{3}. \tag{4.23}$$

4.3. Approximation in an optical lattice potential

For 1D BEC with an optical lattice potential, we choose $d = 1$ and $V_1(x) = \gamma_x^2 x^2/2 + k_x \sin^2(q_x x)$ in (4.2). Then plugging (4.2) into (4.3), after some computations (see Appendix B3), we obtain

$$1 = \int_{-\infty}^{\infty} |\phi_g^{\mathrm{TF}}(x)|^2\, dx \approx \frac{1}{3\beta_1\gamma_x}\left(2\sqrt{(2\mu_g^{\mathrm{TF}})^3} - k_x\sqrt{2\mu_g^{\mathrm{TF}}}\right). \tag{4.24}$$

Solving (4.24), we get

$$\mu_g \approx \mu_g^{\mathrm{TF}} = \frac{1}{2}\left(\frac{3\beta_1\gamma_x}{2}\right)^{2/3} + \frac{k_x}{2}. \tag{4.25}$$

Substituting (4.2) in this case into (2.17), after some computations (see Appendix B3), we obtain

$$E_{\mathrm{int},g} \approx E_{\mathrm{int},g}^{\mathrm{TF}} = \frac{1}{5}\left(\frac{3\beta_1\gamma_x}{2}\right)^{2/3}, \quad E_{\mathrm{pot},g} \approx E_{\mathrm{pot},g}^{\mathrm{TF}} = \frac{1}{10}\left(\frac{3\beta_1\gamma_x}{2}\right)^{2/3} + \frac{k_x}{2}, \tag{4.26}$$

$$E_g \approx E_g^{\mathrm{TF}} = \frac{3}{10}\left(\frac{3\beta_1\gamma_x}{2}\right)^{2/3} + \frac{k_x}{2}, \quad E_{\mathrm{kin},g} \approx E_{\mathrm{kin},g}^{\mathrm{TF}} = 0. \tag{4.27}$$

From (4.25), (4.26) and (4.27), we obtain

$$\lim_{\beta_1\to\infty} \frac{E_g}{\mu_g} = \frac{3}{5}, \qquad \lim_{\beta_1\to\infty} \frac{E_{\mathrm{int},g}}{E_g} = \frac{2}{3}, \qquad \lim_{\beta_1\to\infty} \frac{E_{\mathrm{pot},g}}{E_g} = \frac{1}{3}. \tag{4.28}$$

To verify (4.2) in this case and (4.25)-(4.28) numerically, Table 9 lists the errors between the ground state and its TF approximation and Table 10 lists the energy and chemical potential of the ground and first excited states when we choose $d = 1$ and $V_1(x) = x^2/2 + 25\sin^2(\pi x/4)$ in (2.20). Furthermore, Figure 4 shows the ground and first excited states for different β_1.

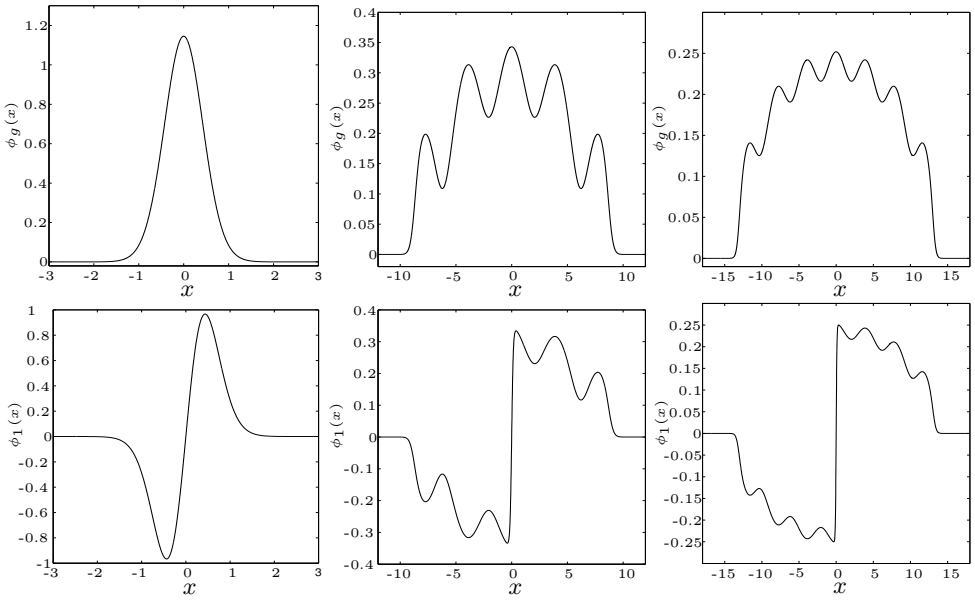

Figure 4. Ground (upper row) and first excited (lower row) states with an optical lattice potential $V_1(x) = x^2/2 + 25\sin^2(\pi x/4)$ for: $\beta_1 = 0$ (left column), $\beta_1 = 400$ (middle column) and $\beta_1 = 1600$ (right column).

Table 9. Convergence study of the TF approximation with an optical lattice potential $V_1(x) = x^2/2 + 25\sin^2(\pi x/4)$.

$1/\beta_1$	1/100	1/400	1/1600	1/3200	1/25600
$\max\|\phi_g - \phi_g^{\rm TF}\|$	0.3963	0.1544	0.0699	0.0366	0.0190
Rate		0.6800	0.5717	0.9334	0.3647
$\|\phi_g - \phi_g^{\rm TF}\|_{L^2}$	0.8257	0.3471	0.1569	0.0952	0.0313
Rate		0.6251	0.5728	0.7208	0.5305
$\|E_{{\rm pot},g} - E_{{\rm pot},g}^{\rm TF}\|$	5.8815	2.2310	0.7943	0.3403	0.0857
Rate		1.1282	0.3160	1.2229	0.5203
$\|E_{{\rm int},g} - E_{{\rm int},g}^{\rm TF}\|$	1.8585	0.6681	0.1102	0.0638	0.0282
Rate		0.7380	1.3000	0.7885	0.8623
$E_{{\rm kin},g} - 0$	0.2928	0.0727	0.0193	0.0103	0.0022
Rate		1.0049	0.9567	0.9060	0.7357
$\|E_g - E_g^{\rm TF}\|$	3.7301	1.4902	0.6648	0.3936	0.1117
Rate		0.6619	0.5823	0.7562	0.6188
$\|\mu_g - \mu_g^{\rm TF}\|$	1.8716	0.8222	0.5547	0.4571	0.1400
Rate		0.6340	0.5934	0.5678	0.1793
E_g/μ_g	0.6967	0.6847	0.6460	0.6316	0.6086
$E_{{\rm int},g}/E_g$	0.4353	0.4604	0.5481	0.5832	0.6433
$E_{{\rm pot},g}/E_g$	0.5477	0.5373	0.4516	0.4167	0.3567

Table 10. Energy and chemical potential of the ground and first excited states with an optical lattice potential $V_1(x) = x^2/2 + 25\sin^2(\pi x/4)$.

β_1	0	25	100	400	1600	6400	25600
E_g	2.7447	9.7896	17.239	32.351	65.612	147.75	353.85
E_1	8.0708	12.382	18.884	33.438	66.468	148.51	354.58
μ_g	2.7447	13.595	24.744	47.247	101.57	237.99	581.46
μ_1	8.0708	15.192	25.868	48.041	102.34	238.72	582.18

From Tables 9 and 10 and Figure 4, the conclusions (1)-(4) in §4.1 are still valid except that we need to replace θ_1, θ_2 by $\theta_1 = 2/5$, $\theta_2 = 2/3$ and the width of the interior layers by $O(1/\beta_1^{1/3})$

4.4. Extension to general case

In d-dimensions with a general potential, e.g. $V_d(\mathbf{x})$ chosen as in (2.25),

plugging (4.2) into (4.3), after some computations (see Appendix B4), we obtain

$$1 = \int_{\mathbb{R}^d} |\phi_g^{\rm TF}(\mathbf{x})|^2 d\mathbf{x} \approx \frac{(2\mu_g^{\rm TF})^{(\alpha+d)/\alpha}}{2\beta_d \prod_{j=1}^d \gamma_{x_j}} \, C_{\alpha,d}, \tag{4.29}$$

where $C_{\alpha,d}$ is given in (B.11). Solving (4.29), we get

$$\mu_g^{\rm TF} = \frac{1}{2} \left(\frac{2\beta_d \prod_{j=1}^d \gamma_{x_j}}{C_{\alpha,d}} \right)^{\alpha/(\alpha+d)}. \tag{4.30}$$

Plugging (4.2) into (2.17), after some computations (see Appendix B4), we get

$$E_{{\rm int},g} \approx E_{{\rm int},g}^{\rm TF} = \frac{D_{\alpha,d}}{4C_{\alpha,d}} \left(\frac{2\beta_d \prod_{j=1}^d \gamma_{x_j}}{C_{\alpha,d}} \right)^{\alpha/(\alpha+d)}, \tag{4.31}$$

$$E_{{\rm pot},g} \approx E_{{\rm pot},g}^{\rm TF} = \frac{C_{\alpha,d} - D_{\alpha,d}}{2C_{\alpha,d}} \left(\frac{2\beta_d \prod_{j=1}^d \gamma_{x_j}}{C_{\alpha,d}} \right)^{\alpha/(\alpha+d)}, \tag{4.32}$$

$$E_g \approx E_g^{\rm TF} = \frac{G_{\alpha,d}}{4C_{\alpha,d}} \left(\frac{2\beta_d \prod_{j=1}^d \gamma_{x_j}}{C_{\alpha,d}} \right)^{\alpha/(\alpha+d)}, \quad G_{\alpha,d} = 2C_{\alpha,d} - D_{\alpha,d}, \tag{4.33}$$

where $D_{\alpha,d}$ is given in (B.13). From (4.30), (4.31), (4.32) and (4.33), we obtain

$$\lim_{\beta_d \to \infty} \frac{E_g}{\mu_g} = \frac{G_{\alpha,d}}{2C_{\alpha,d}}, \quad \lim_{\beta_d \to \infty} \frac{E_{{\rm int},g}}{E_g} = \frac{D_{\alpha,d}}{G_{\alpha,d}}, \quad \lim_{\beta_d \to \infty} \frac{E_{{\rm pot},g}}{E_g} = \frac{2(C_{\alpha,d} - D_{\alpha,d})}{G_{\alpha,d}}. \tag{4.34}$$

5. Conclusion

We presented asymptotic approximations up to $o(1)$ in term of the scaled interacting parameter β_d for the energy and chemical potential, as well as their ratio, of the ground state in Bose-Einstein condensates in the semiclassical regime with several typical trapping potentials. For a uniform box potential, the approximations were obtained by a matched asymptotic method; while for nonuniform potentials, e.g. harmonic oscillator, double well and optical lattice potentials, they were derived from the TF approximation. These asymptotic approximations were confirmed by our extensive numerical results.

Furthermore, based on our asymptotic and extensive numerical studies for the nonlinear eigenvalue problem (2.20)-(2.22) with $\beta_d \geq 0$, Ω is bounded (or Ω is unbounded but $\lim_{|\mathbf{x}|\to\infty} V_d(\mathbf{x}) = \infty$), we can draw the following conjectures:

(i) It admits infinitely many eigenfunctions which are linearly independent.

(ii) If all the eigenfunctions are ranked according to their energies, ϕ_g, ϕ_1, $\cdots$, then the corresponding eigenvalues (or chemical potentials) are in the same order, i.e.

$$E(\phi_g) \leq E(\phi_1) \leq E(\phi_2) \leq \cdots \quad \Longrightarrow \quad \mu(\phi_g) \leq \mu(\phi_1) \leq \mu(\phi_2) \leq \cdots .$$

(iii) When $\beta_d \to \infty$, the ratios between energy and chemical potential are constants, i.e.

$$\lim_{\beta_d\to\infty} \frac{E(\phi_g)}{\mu(\phi_g)} = \text{const}, \ \lim_{\beta_d\to\infty} \frac{E(\phi_k)}{E(\phi_g)} = 1, \ \lim_{\beta_d\to\infty} \frac{\mu(\phi_k)}{\mu(\phi_g)} = 1, \ k \in \mathbb{N}.$$

(iv) When Ω is bounded, in the semiclassical regime, i.e. $\beta_d \gg 1$, boundary layers with width $O(1/\sqrt{\beta_d})$ are observed at $\partial\Omega$ in both the ground and excited states, and interior layers with width $O(1/\sqrt{\beta_d})$ are observed in the excited states. When $\Omega = \mathbb{R}^d$ and $V(\mathbf{x})$ is chosen as (2.25), interior layers with width $O(1/\beta_d^{(2+\alpha)/4(\alpha+d)})$ are observed in the excited states.

(v) For box potentials, the CNGF and its BEFD discretization, proposed in [6], can be directly applied to compute the ground and all excited states provided appropriate initial data is chosen; for nonuniform even potentials, it can only be directly applied to compute the ground and first excited states provided that the initial data is chosen as even and odd functions respectively.

Appendix A. Computations for 1D box potential in §3

A.1. For ground state in §3.3

Plugging (3.17) into (2.22), we obtain

$$\begin{aligned} 1 &= \int_0^1 |\phi_g^{\mathrm{MA}}(x)|^2 \, dx \\ &= \frac{\mu_g^{\mathrm{MA}}}{\beta_1} \left[\int_0^1 \tanh^2\left(\sqrt{\mu_g^{\mathrm{MA}}} x\right) dx + \int_0^1 \tanh^2\left(\sqrt{\mu_g^{\mathrm{MA}}}(1-x)\right) dx \right. \end{aligned}$$

$$
\begin{aligned}
&-2\tanh\left(\sqrt{\mu_g^{\rm MA}}\right)\int_0^1\left[\tanh\left(\sqrt{\mu_g^{\rm MA}}x\right)+\tanh\left(\sqrt{\mu_g^{\rm MA}}(1-x)\right)\right]dx\\
&+2\int_0^1\tanh\left(\sqrt{\mu_g^{\rm MA}}x\right)\tanh\left(\sqrt{\mu_g^{\rm MA}}(1-x)\right)dx+\tanh^2\left(\sqrt{\mu_g^{\rm MA}}\right)\Bigg]dx\\
=&\ \frac{\mu_g^{\rm MA}}{\beta_1}\Bigg[2\left(1-\frac{\tanh\left(\sqrt{\mu_g^{\rm MA}}\right)}{\sqrt{\mu_g^{\rm MA}}}\right)-4\tanh\left(\sqrt{\mu_g^{\rm MA}}\right)\frac{\ln\left(\cosh\left(\sqrt{\mu_g^{\rm MA}}\right)\right)}{\sqrt{\mu_g^{\rm MA}}}\\
&+2\left(-1+2\frac{\coth\left(\sqrt{\mu_g^{\rm MA}}\right)\ln\left(\cosh\left(\sqrt{\mu_g^{\rm MA}}\right)\right)}{\sqrt{\mu_g^{\rm MA}}}\right)+\tanh^2\left(\sqrt{\mu_g^{\rm MA}}\right)\Bigg]\\
\approx&\ \frac{\mu_g^{\rm MA}}{\beta_1}\Big[2\Big(1-\frac{1}{\sqrt{\mu_g^{\rm MA}}}\Big)-4\frac{\sqrt{\mu_g^{\rm MA}}-\ln 2}{\sqrt{\mu_g^{\rm MA}}}+2\Big(-1+2\frac{\sqrt{\mu_g^{\rm MA}}-\ln 2}{\sqrt{\mu_g^{\rm MA}}}\Big)+1\Big]\\
=&\ \frac{\mu_g^{\rm MA}}{\beta_1}\Big(1-\frac{2}{\sqrt{\mu_g^{\rm MA}}}\Big)=\frac{\mu_g^{\rm MA}}{\beta_1}-2\frac{\sqrt{\mu_g^{\rm MA}}}{\beta_1},
\end{aligned}
\tag{A.1}
$$

here we use $e^{-\alpha}\approx 0$ when $\alpha\gg 1$. Similarly, plugging (3.17) into (2.17), we obtain

$$
\begin{aligned}
E_{{\rm kin},g}^{\rm MA}=E_{\rm kin}(\phi_g^{\rm MA})=&\frac{1}{2}\int_0^1\left|\left[\phi_g^{\rm MA}(x)\right]'\right|^2dx\\
=&\ \frac{(\mu_g^{\rm MA})^2}{2\beta_1}\int_0^1\left[\operatorname{sech}^2\left(\sqrt{\mu_g^{\rm MA}}x\right)-\operatorname{sech}^2\left(\sqrt{\mu_g^{\rm MA}}(1-x)\right)\right]^2dx\\
=&\ \frac{(\mu_g^{\rm MA})^2}{2\beta_1}\int_0^1\Bigg[\operatorname{sech}^4\left(\sqrt{\mu_g^{\rm MA}}x\right)+\operatorname{sech}^4\left(\sqrt{\mu_g^{\rm MA}}(1-x)\right)\\
&-2\operatorname{sech}^2\left(\sqrt{\mu_g^{\rm MA}}x\right)\operatorname{sech}^2\left(\sqrt{\mu_g^{\rm MA}}(1-x)\right)\Bigg]dx\\
=&\ \frac{(\mu_g^{\rm MA})^2}{2\beta_1}\Bigg[\frac{2}{\sqrt{\mu_g^{\rm MA}}}\Bigg(-2\coth\left(\sqrt{\mu_g^{\rm MA}}\right)\operatorname{csch}^2\left(\sqrt{\mu_g^{\rm MA}}\right)\ln\left(\cosh\left(\sqrt{\mu_g^{\rm MA}}\right)\right)\\
&+\operatorname{csch}\left(\sqrt{\mu_g^{\rm MA}}\right)\operatorname{sech}\left(\sqrt{\mu_g^{\rm MA}}\right)\Bigg)+\frac{2\tanh\left(\sqrt{\mu_g^{\rm MA}}\right)\left(2+\operatorname{sech}^2\left(\sqrt{\mu_g^{\rm MA}}\right)\right)}{3\sqrt{\mu_g^{\rm MA}}}\Bigg]\\
\approx&\ \frac{2}{3}\frac{\mu_g^{\rm MA}\sqrt{\mu_g^{\rm MA}}}{\beta_1}.
\end{aligned}
\tag{A.2}
$$

Thus (3.20) is a combination of (A.2) and (3.19). Furthermore, (3.21) and (3.22) can be derived from (3.19), (3.20) and (3.1) with $\phi = \phi_g^{\mathrm{MA}}$.

A.2. For excited states in §3.4

Plugging (3.24) into (2.22), we obtain

$$\begin{aligned}
1 \;=\; & \int_0^1 |\phi_k^{\mathrm{MA}}(x)|^2\,dx \\
\approx\; & \frac{\mu_k^{\mathrm{MA}}}{\beta_1}\Bigg\{ \sum_{j=0}^{[(k+1)/2]} \Big(1-\frac{2}{\sqrt{\mu_k^{\mathrm{MA}}}}\Big) + \sum_{j=0}^{[k/2]} \Big(1-\frac{2}{\sqrt{\mu_k^{\mathrm{MA}}}}\Big) \\
& +2\sum_{j=0}^{[(k+1)/2]}\sum_{s=j+1}^{[(k+1)/2]} \Big[1-\frac{4(s-j)}{k+1}\Big] \\
& +2\sum_{j=0}^{[(k+1)/2]} \Bigg[\sum_{s=0}^{j}\Big[-1+\frac{2[2(j-s)-1]}{k+1}\Big] + \sum_{s=j+1}^{[k/2]}\Big[-1+\frac{2\,[2(s-j)+1]}{k+1}\Big]\Bigg] \\
& +C_k^2 - 2C_k\Bigg[\sum_{j=0}^{[(k+1)/2]}\Big(1-\frac{4j}{k+1}\Big) + \sum_{j=0}^{[k/2]}\Big[-1+\frac{2\,(2j+1)}{k+1}\Big]\Bigg] \\
& +2\sum_{j=0}^{[k/2]}\sum_{s=j+1}^{[k/2]}\Big[1-\frac{4(s-j)}{k+1}\Big]\Bigg\} \\
\approx\; & \frac{\mu_k^{\mathrm{MA}}}{\beta_1}\Big(1-\frac{2(k+1)}{\sqrt{\mu_k^{\mathrm{MA}}}}\Big). \qquad \text{(A.3)}
\end{aligned}$$

Similarly, plugging (3.24) into (2.17), we obtain

$$\begin{aligned}
E_{\mathrm{kin},k}^{\mathrm{MA}} \;=\; & E_{\mathrm{kin}}(\phi_k^{\mathrm{MA}}) = \frac{1}{2}\int_0^1 |[\phi_k^{\mathrm{MA}}(x)]'|^2\,dx \\
=\; & \frac{\big(\mu_k^{\mathrm{MA}}\big)^2}{2\beta_1}\int_0^1 \Bigg[\sum_{j=0}^{[(k+1)/2]} \operatorname{sech}^2\Big(\sqrt{\mu_k^{\mathrm{MA}}}\Big(x-\frac{2j}{k+1}\Big)\Big) \\
& \qquad + \sum_{j=0}^{[k/2]} \operatorname{sech}^2\Big(\sqrt{\mu_k^{\mathrm{MA}}}\Big(\frac{2j+1}{k+1}-x\Big)\Big)\Bigg]^2 dx \\
=\; & \frac{\big(\mu_k^{\mathrm{MA}}\big)^2}{2\beta_1}\left(\sum_{j=0}^{[(k+1)/2]}\frac{4}{3\sqrt{\mu_k^{\mathrm{MA}}}} + \sum_{j=0}^{[k/2]}\frac{4}{3\sqrt{\mu_k^{\mathrm{MA}}}}\right)
\end{aligned}$$

$$= \frac{2(k+1)\mu_k^{\mathrm{MA}}\sqrt{\mu_k^{\mathrm{MA}}}}{3\beta_1}. \tag{A.4}$$

Thus (3.27) is a combination of (A.4) and (3.26). Furthermore, (3.28) and (3.29) can be derived from (3.26), (3.27) and (3.1) with $\phi = \phi_k^{\mathrm{MA}}$.

Appendix B. Computations for nonuniform potentials in §4

B.1. For 1D harmonic oscillator potential in §4.1

Plugging (4.2) with $d = 1$ and $V_1(x) = \gamma_x^2 x^2/2$ into (4.3) and using change of variable $x = \frac{\sqrt{2\mu_g^{TF}}}{\gamma_x}t$, we obtain

$$\begin{aligned} 1 &= \int_{-\infty}^{\infty} |\phi_g^{\mathrm{TF}}(x)|^2\, dx = \int_{\gamma_x^2 x^2 \le 2\mu_g^{\mathrm{TF}}} \frac{\mu_g^{\mathrm{TF}} - \frac{1}{2}\gamma_x^2 x^2}{\beta_1}\, dx \\ &= \frac{\sqrt{2\mu_g^{\mathrm{TF}}}}{\beta_1\gamma_x}\int_{-1}^{1}\left(\mu_g^{\mathrm{TF}} - \mu_g^{\mathrm{TF}} t^2\right)\, dt = \frac{2}{3}\frac{\left(2\mu_g^{\mathrm{TF}}\right)^{3/2}}{\beta_1\gamma_x}. \end{aligned} \tag{B.1}$$

Similarly, plugging (4.2) with the setup into (2.17), we obtain

$$E_{\mathrm{int},g}^{\mathrm{TF}} = \frac{\beta_1}{2}\int_{\gamma_x^2 x^2 \le 2\mu_g^{\mathrm{TF}}}\left(\frac{\mu_g^{\mathrm{TF}} - \frac{1}{2}\gamma_x^2 x^2}{\beta_1}\right)^2 dx = \frac{4}{15}\frac{\left(2\mu_g^{\mathrm{TF}}\right)^{5/2}}{\beta_1\gamma_x}. \tag{B.2}$$

$$E_{\mathrm{pot},g}^{\mathrm{TF}} = \int_{\gamma_x^2 x^2 \le 2\mu_g^{\mathrm{TF}}} \frac{\gamma_x^2 x^2\left(\mu_g^{\mathrm{TF}} - \frac{1}{2}\gamma_x^2 x^2\right)}{2\beta_1}\, dx = \frac{2}{15}\frac{\left(2\mu_g^{\mathrm{TF}}\right)^{5/2}}{\beta_1\gamma_x}. \tag{B.3}$$

Thus (4.8) is a combination of (4.7) and (B.3). Furthermore, (4.9) is a combination of (4.8), (4.4) and (4.5).

B.2. For 1D double well potential in §4.2

Plugging (4.2) with $d = 1$ and $V_1(x) = \gamma_x^4(x^2 - a^2)^2/2$ into (4.3) and using change of variable $x = \frac{1}{\gamma_x}\sqrt{a^2\gamma_x^2 + \sqrt{2\mu_g^{TF}}t}$, we obtain

$$1 = \int_{-\infty}^{\infty} |\phi_g^{\mathrm{TF}}(x)|^2\, dx = \int_{\gamma_x^4(x^2-a^2)^2 \le 2\mu_g^{\mathrm{TF}}}\left(\frac{\mu_g^{\mathrm{TF}} - \frac{1}{2}\gamma_x^4\left(x^2 - a^2\right)^2}{\beta_1}\right) dx$$

$$= \frac{1}{\beta_1\gamma_x}\sqrt{a^2\gamma_x^2+\sqrt{2\mu_g^{\rm TF}}}\int_{-1}^{1}\left[\mu_g^{\rm TF}-\frac{1}{2}\left(\left(\sqrt{2\mu_g^{\rm TF}}+a^2\gamma_x^2\right)t^2-a^2\gamma_x^2\right)^2\right]dt$$
$$= \frac{4}{15\beta_1\gamma_x}\left(6\mu_g^{\rm TF}+a^2\gamma_x^2\sqrt{2\mu_g^{\rm TF}}-2a^4\gamma_x^4\right)\sqrt{a^2\gamma_x^2+\sqrt{2\mu_g^{\rm TF}}}. \quad \text{(B.4)}$$

Similarly, plugging (4.2) with the setup into (2.17) and using change of variable, we get

$$E_{{\rm int},g}^{\rm TF} = \frac{\beta_1}{2}\int_{\gamma_x^4(x^2-a^2)^2\le 2\mu_g^{\rm TF}}\left(\frac{\mu_g^{\rm TF}-\frac{1}{2}\gamma_x^4\left(x^2-a^2\right)^2}{\beta_1}\right)^2 dx$$
$$= \frac{1}{8\beta_1\gamma_x}\left[\frac{64}{45}\left(2\mu_g^{\rm TF}\right)^2-\frac{704}{315}a^2\gamma_x^2\left(\sqrt{2\mu_g^{\rm TF}}\right)^3+\frac{128}{21}a^4\gamma_x^4\left(2\mu_g^{\rm TF}\right)\right.$$
$$\left.+\frac{1024}{315}a^6\gamma_x^6\sqrt{2\mu_g^{\rm TF}}+\frac{472}{315}a^8\gamma_x^8\right]\sqrt{a^2\gamma_x^2+\sqrt{2\mu_g^{\rm TF}}}. \quad \text{(B.5)}$$

$$E_{{\rm pot},g}^{\rm TF} = \int_{\gamma_x^4(x^2-a^2)^2\le 2\mu_g^{\rm TF}}\frac{\gamma_x^4(x^2-a^2)^2\left(\mu_g^{\rm TF}-\frac{1}{2}\gamma_x^4\left(x^2-a^2\right)^2\right)}{2\beta_1}dx$$
$$= \frac{1}{4\beta_1\gamma_x}\left[\frac{4}{45}\left(2\mu_g^{\rm TF}\right)^2-\frac{44}{315}a^2\gamma_x^2\left(\sqrt{2\mu_g^{\rm TF}}\right)^3+\frac{8}{21}a^4\gamma_x^4\left(2\mu_g^{\rm TF}\right)\right.$$
$$\left.+\frac{64}{315}a^6\gamma_x^6\sqrt{2\mu_g^{\rm TF}}-\frac{128}{315}a^8\gamma_x^8\right]\sqrt{a^2\gamma_x^2+\sqrt{2\mu_g^{\rm TF}}}. \quad \text{(B.6)}$$

Thus (4.13) is a combination of (4.12) and (B.5), and (4.14) is a combination of (4.12) and (B.6). Furthermore, combining (4.13)), (4.12), (4.14), (4.4) and (4.5), we get (4.15) and (4.16) immediately.

B.3. For 1D optical lattice potential in §4.3

Plugging (4.2) with $d=1$ and $V_1(x)=\gamma_x^2x^2/2+k_x\sin^2(q_xx)$ into (4.3), we get

$$1 = \int_{-\infty}^{\infty}|\phi_g^{\rm TF}(x)|^2\,dx$$
$$= \frac{1}{\beta_1}\int_{\frac{1}{2}\gamma_x^2x^2+k_x\sin^2(q_xx)\le\mu_g^{\rm TF}}\left[\mu_g^{\rm TF}-\left(\frac{1}{2}\gamma_x^2x^2+k_x\sin^2(q_xx)\right)\right]dx$$

$$\begin{aligned}
&\approx \frac{1}{\beta_1}\int_{\gamma_x^2x^2\le 2\mu_g^{\rm TF}}\left[\mu_g^{\rm TF}-\left(\frac{1}{2}\gamma_x^2x^2+k_x\sin^2(q_xx)\right)\right]dx\\
&\overset{x=\frac{\sqrt{2\mu_g^{\rm TF}}}{\gamma_x}t}{=} \frac{\sqrt{2\mu_g^{\rm TF}}}{\beta_1\gamma_x}\int_{-1}^{1}\left[\mu_g^{\rm TF}-\left(\mu_g^{\rm TF}t^2+k_x\sin^2\left(\frac{q_x\sqrt{2\mu_g^{\rm TF}}}{\gamma_x}t\right)\right)\right]dt\\
&\approx \frac{1}{3\beta_1\gamma_x}\left[2\sqrt{(2\mu_g^{\rm TF})^3}-k_x\sqrt{2\mu_g^{\rm TF}}\right]. \qquad \text{(B.7)}
\end{aligned}$$

Similarly, substituting (4.2) with the setup into (2.17), we obtain

$$\begin{aligned}
E_{{\rm int},g}^{\rm TF} &= !\frac{1}{2\beta_1}\int_{\frac{1}{2}\gamma_x^2x^2+k_x\sin^2(q_xx)\le\mu_g^{\rm TF}}\left[\mu_g^{\rm TF}-\left(\frac{1}{2}\gamma_x^2x^2+k_x\sin^2(q_xx)\right)\right]^2dx\\
&\approx \frac{1}{2\beta_1}\int_{\gamma_x^2x^2\le 2\mu_g^{\rm TF}}\left[\mu_g^{\rm TF}-\left(\frac{1}{2}\gamma_x^2x^2+k_x\sin^2(q_xx)\right)\right]^2dx\\
&= \frac{1}{4\beta_1\gamma_x}\left[\frac{1}{30}\left(\sqrt{2\mu_g^{\rm TF}}\right)^5-\frac{k_x}{12}\left(\sqrt{2\mu_g^{\rm TF}}\right)^3+\left(\frac{3k_x^2}{2}-\frac{k_x\gamma_x^2}{q_x^2}\right)\sqrt{2\mu_g^{\rm TF}}\right.\\
&\quad\left.+\frac{k_x^2\gamma_x}{8q_x}\sin\left(\frac{4q_x\sqrt{2\mu_g^{\rm TF}}}{\gamma_x}\right)+\left(\frac{k_x\gamma_x^3}{q_x}-\frac{k_x^2\gamma_x}{q_x}\right)\sin\left(\frac{2q_x\sqrt{2\mu_g^{\rm TF}}}{\gamma_x}\right)\right]. \qquad \text{(B.8)}
\end{aligned}$$

$$\begin{aligned}
E_{{\rm pot},g}^{\rm TF} &= \int_{V_1(x)\le\mu_g^{\rm TF}}\frac{\left(\gamma_x^2x^2+2k_x\sin^2(q_xx)\right)\left(\mu_g^{TF}-\left(\frac{1}{2}\gamma_x^2x^2+k_x\sin^2(q_xx)\right)\right)}{2\beta_1}dx\\
&\approx \int_{\gamma_x^2x^2\le 2\mu_g^{\rm TF}}\frac{\left(\gamma_x^2x^2+2k_x\sin^2(q_xx)\right)\left(\mu_g^{\rm TF}-\left(\frac{1}{2}\gamma_x^2x^2+k_x\sin^2(q_xx)\right)\right)}{2\beta_1}\,dx\\
&\approx \frac{1}{60\beta_1\gamma_x}\left(4\left(\sqrt{2\mu_g^{\rm TF}}\right)^5+10k_x\left(2\mu_g^{\rm TF}\right)+45k_x^2\right). \qquad \text{(B.9)}
\end{aligned}$$

Thus (4.26) is a combination of (4.25), (B.9) and (B.8). Furthermore, combining (4.26), (4.25), (4.4) and (4.5), we get (4.27) immediately.

B4. For general potential in §4.4

Plugging (4.2) into (4.3) and using change of variables, we obtain

$$\begin{aligned}
1 &= \int_{\mathbb{R}^d}|\phi_g^{\rm TF}(\mathbf{x})|^2d\mathbf{x}=\int_{V_d(\mathbf{x})\le\mu_g^{\rm TF}}\frac{\mu_g^{\rm TF}-V_d(\mathbf{x})}{\beta_d}d\mathbf{x}\\
&\approx \int_{V_0(\mathbf{x})\le\mu_g^{\rm TF}}\frac{\mu_g^{\rm TF}-V_0(\mathbf{x})}{\beta_d}d\mathbf{x}=\int_{\sum_{j=1}^d\gamma_{x_j}^\alpha|x_j|^\alpha\le 2\mu_g^{\rm TF}}\frac{\mu_g^{\rm TF}-\sum_{j=1}^d\gamma_{x_j}^\alpha|x_j|^\alpha}{\beta_d}d\mathbf{x}
\end{aligned}$$

$$= \frac{(2\mu_g^{\mathrm{TF}})^{(\alpha+d)/\alpha}}{2\beta_d \prod_{j=1}^d \gamma_{x_j}} C_{\alpha,d}, \tag{B.10}$$

where

$$C_{\alpha,d} = \int_{\sum_{j=1}^d |x_j|^\alpha \le 1} \left(1 - 2\sum_{j=1}^d |x_j|^\alpha\right) d\mathbf{x}. \tag{B.11}$$

Similarly, plugging (4.2) into (2.17), we obtain

$$\begin{aligned} E_{\mathrm{int},g}^{\mathrm{TF}} &= \int_{V_d(\mathbf{x}) \le \mu_g^{\mathrm{TF}}} \frac{[\mu_g^{\mathrm{TF}} - V_d(\mathbf{x})]^2}{2\beta_d} d\mathbf{x} \\ &\approx \int_{\sum_{j=1}^d \gamma_{x_j}^\alpha |x_j|^d \le 2\mu_g^{\mathrm{TF}}} \frac{[\mu_g^{\mathrm{TF}} - V_0(\mathbf{x})]^2}{2\beta_d} d\mathbf{x} = \frac{(2\mu_g^{\mathrm{TF}})^{(2\alpha+d)/\alpha}}{8\beta_d \prod_{j=1}^d \gamma_{x_j}} D_{\alpha,d}, \end{aligned} \tag{B.12}$$

where

$$D_{\alpha,d} = \int_{\sum_{j=1}^d |x_j|^\alpha \le 1} \left(1 - 2\sum_{j=1}^d |x_j|^\alpha\right)^2 d\mathbf{x}. \tag{B.13}$$

$$\begin{aligned} E_{\mathrm{pot},g}^{\mathrm{TF}} &= \int_{V_d(\mathbf{x}) \le \mu_g^{\mathrm{TF}}} V_d(\mathbf{x}) \frac{\mu_g^{\mathrm{TF}} - V(\mathbf{x})}{\beta_d} d\mathbf{x} \approx \int_{V_0(\mathbf{x}) \le \mu_g^{\mathrm{TF}}} V_0(\mathbf{x}) \frac{\mu_g^{\mathrm{TF}} - V_0(\mathbf{x})}{\beta_d} d\mathbf{x} \\ &= \frac{(2\mu_g^{\mathrm{TF}})^{(2\alpha+d)/\alpha}}{4\beta_d \prod_{j=1}^d \gamma_{x_j}} \int_{\sum_{j=1}^d |x_j|^\alpha \le 1} \left(\sum_{j=1}^d |x_j|^\alpha\right)\left(1 - 2\sum_{j=1}^d |x_j|^\alpha\right) d\mathbf{x} \\ &= \frac{(2\mu_g^{\mathrm{TF}})^{(2\alpha+d)/\alpha}}{4\beta_d \prod_{j=1}^d \gamma_{x_j}} \left(C_{\alpha,d} - D_{\alpha,d}\right). \end{aligned} \tag{B.14}$$

Thus (4.31) is a combination of (4.30) and (B.12), (4.32) is a combination of (4.30) and (B.14). Furthermore, combining (4.31), (4.30), (4.4), we get (4.33) immediately.

Acknowledgment

The authors acknowledge support by the National University of Singapore grant No. R-146-000-081-112. The work was partially done while the first author was visiting the Institute for Mathematical Sciences, National University of Singapore in 2005.

References

1. J. R. Abo-Shaeer, C. Raman, J. M. Vogels and W. Ketterle, Observation of vortex lattices in Bose-Einstein condensates, *Science*, **292**(2001), 476-479.

2. S. K. Adhikari and P. Muruganandam, Mean-field model for the interference of matter-waves from a three-dimensional optical trap, *Phys. Lett. A*, **310**(2003), 229-235.

3. M. H. Anderson, J. R. Ensher, M. R. Matthewa, C. E. Wieman and E. A. Cornell, Observation of Bose-Einstein condensation in a dilute atomic vapor, *Science*, **269**(1995), 198-201.

4. J. R. Anglin and W. Ketterle, Bose-Einstein condensation of atomic gases, *Nature*, **416** (2002), 211-218.

5. W. Bao, Ground states and dynamics of multi-component Bose-Einstein condensates, *Multiscale Model. Simul.*, **2**(2004), 210-236.

6. W. Bao and Q. Du, Computing the ground state solution of Bose-Einstein condensates by a normalized gradient flow, *SIAM J. Sci. Comput.*, **25** (2004), 1674-1697.

7. W. Bao and D. Jaksch, An explicit unconditionally stable numerical method for solving damped nonlinear Schrodinger equations with a focusing nonlinearity, *SIAM J. Numer. Anal.*, **41**(2003), 1406-1426.

8. W. Bao, D. Jaksch and P.A. Markowich, Numerical solution of the Gross-Pitaevskii equation for Bose-Einstein condensation, *J. Comput. Phys.*, **187**(2003), 318-342.

9. W. Bao, D. Jaksch and P. A. Markowich, Three dimensional simulation of jet formation in collapsing condensates, *J. Phys. B: At. Mol. Opt. Phys.*, **37**(2004), 329-343.

10. W. Bao and J. Shen, A Fourth-order time-splitting Laguerre-Hermite pseudospectral method for Bose-Einstein condensates, *SIAM J. Sci. Comput.*, **26**(2005), 2010-2028.

11. W. Bao and W.J. Tang, Ground state solution of trapped interacting Bose-Einstein condensate by directly minimizing the energy functional, *J. Comput. Phys.*, **187**(2003), 230-254.

12. W. Bao and Y. Z. Zhang, Dynamics of the ground state and central vortex states in Bose-Einstein condenstation, *Math. Models Methods Appl. Sci.*, **15**(2005), 1863-1896.

13. G. Baym and C.J. Pethick, Ground-state properties of magnetically trapped Bose-condensed Rubidium gas, *Phys. Rev. Lett.*, **76**(1996), 6-9.

14. C.C. Bradley, C. A. Sackett, R. G. Hulet, Bose-Einstein condensation of Lithium: observation of limited condensates, *Phys. Rev. Lett.*, **78**(1997), 985-989.

15. J. C. Bronski, L. D. Carr, B. Deconinck, J. N. Kutz and K. Promislow, Stability of repulsive Bose-Einstein condensates in a periodic potential, *Phys. Rev. E*, **63**(2001), 036612.

16. P. Capuzzi and S. Hernandez, Bose-Einstein condensation in harmonic double wells, *Phys. Rev. A*, **59**(1999), 1488.

17. R. Carles, P. A. Markowich and C, Sparber, Semiclassical asymptotics for weakly nonlinear bloch waves, preprint.

18. L.D. Carr, Charles W. Clark and W.P. Reinhardt, Stationary solutions of the one-dimensional nonlinear Schrodinger equation I. case of repulsive nonlinearity, *Phys. Rev. A*, **62**(2000), 063610.

19. M.M. Cerimele, M.L. Chiofalo, F. Pistella, S. Succi and M.P. Tosi, Numerical solution of the Gross-Pitaevskii equation using an explicit finite-difference scheme: An application to trapped Bose-Einstein condensates, *Phys. Rev. E*, **62**(2000), 1382-1389.

20. S.-M. Chang, W.-W. Lin and S.-F., Shieh, Gauss-Seidel-type methods for energy states of a multi-component Bose-Einstein condensate, *J. Comput. Phys.*, **202**(2005), 367-390.

21. M. L. Chiofalo, S. Succi and M. P. Tosi, Ground state of trapped interacting Bose-Einstein condensates by an explicit imaginary-time algorithm, *Phys. Rev. E*, **62**(2000), 7438-7444.

22. D.-I. Choi and Q. Niu, Bose-Einstein condensates in an optical latice, *Phys. Rev. Lett.*, **82**(1999), 2022-2025.

23. E. Cornell, Very cold indeed: The nanokelvin physics of Bose-Einstein condensation, *J. Res. Natl. Inst. Stan.*, **101**(1996), 419-434.

24. F. Dalfovo, S. Giorgini, L. P. Pitaevskii and S. Stringari, Theory of Bose-Einstein condensation in trapped gases, *Rev. Modern Phys.*, **71**(1999), 463-512.

25. K.B. Davis, M.O. Mewes, M.R. Andrews, N.J. van Druten, D.S. Durfee, D.M. Kurn and W. Ketterle, Bose-Einstein condenstion in a gas of sodium atoms, *Phys. Rev. Lett.*, **75**(1995), 3969-3973.

26. R. Dum, J.I. Cirac, M. Lewenstein and P. Zoller, Creation of dark solitons and vortices in Bose-Einstein condensates, *Phys. Rev. Lett.*, **80**(1998), 2972-2975.

27. M. Edwards, P. A. Ruprecht and K. Burnett, R. J. Dodd and C.W. Clark, Collective excitations of atomic Bose-Einstein condensates, *Phys. Rev. Lett.*, **77**(1996), 1671-1674.

28. M. Greiner, O. Mandel, T. Esslinger, T. W. Hänsch and I. Bloch, Quantum phase transition from a superfluid to a mott insulator in a gas of ultracold atoms, *Nature*, **415**(2002), 39-45.

29. E. P. Gross, Structure of a quantized vortex in boson systems, *Nuovo. Cimento.*, **20**(1961), 454-477.

30. M. Holthaus, Towards coherent control of a Bose-Einstein condensate in a double well, *Phys. Rev. A*, **64**(2001), 011601.

31. D. A. W. Hutchinson, E. Zaremba and A. Griffin, Finite temperature excitations of a trapped bose gas, *Phys. Rev. Lett.*, **78** (1997), 1842-1845.

32. D. S. Jin, J. R. Ensher, M. R. Matthews, C. E. Wiemann and E. A. Cornell, Collective excitations of a Bose-Einstein condensate in a dilute gas, *Phys. Rev. Lett.*, **77**(1996), 420-423.

33. L. Laudau and E. Lifschitz, Quantum Mechanics: non-relativistic theory, Pergamon Press, New York, 1977.

34. P. Leboeuf and N. Pavloff, Bose-Einstein beams: coherent propagation through a guide, *Phys. Rev. A*, **64**(2001), 033602;

35. E.H. Lieb and R. Seiringer, One-dimensional bosons in three-dimensional traps, *Phys. Rev. Lett.*, **91** (2003), 150401.

36. E. H. Lieb, R. Seiringer and J. Yugvason, Bosons in a trap: a rigorous derivation of the Gross-Pitaevskii energy functional, *Phys. Rev. A*, **61**(2000), 3602.

37. F.Y. Lim, Numerical Simulation for Bose-Einstein Condensation, B. Sc. (Honours) Thesis, Department of Computational Science, National University of Singapore, 2004.

38. G.J. Milburn, J. Corney, E.M. Wright and D.F. Walls, Quantum dynamics of an atomic Bose-Einstein condensate in a double-well potential, *Phys. Rev. A*, **55**(1997), 4318.

39. C.J. Pethick and H. Smith, Bose-Einstein Condensation in Dilute Gases, Cambridge Unversity Press, 2002.

40. L. P. Pitaevskii, Vortex lines in a imperfect Bose gase, *Zh. Eksp. Teor. Fiz.*, **40**(1961), 646-649. (*Sov. Phys. JETP*, **13**(1961), 451-454).

41. L. P. Pitaevskii and S. Stringari, Bose-Einstein condensation, Clarendon press, 2003.

42. D. S. Rokhsar, Vortex stability and persistent currents in trapped bose gas, *Phys. Rev. Lett.*, **79**(1997), 2164-2167.

43. C. Sparber, Effective mass theorems for nonlinear Schrödinger equations, preprint.

Department of Mathematics and Center for Computational Science and Engineering, National University of Singapore, 117543, Singapore.

E-mail: bao@math.nus.edu.sg

Department of Mathematics and Center for Computational Science and Engineering, National University of Singapore, 117543, Singapore.

E-mail: fongyin.lim@nus.edu.sg

Department of Mathematics and Center for Computational Science and Engineering, National University of Singapore,

E-mail: zhyanzhi@nus.edu.sg